

## Two-Pion Exchange in Proton-Proton Scattering

**W. R. Gibbs**

New Mexico State University, Las Cruces NM 88003

and

**B. Loiseau**

LPNHE-Laboratoire de Physique Nucléaire et de Hautes Énergies, Groupe Théorie,  
IN2P3-CNRS, Universités P. & M. Curie et Denis Diderot, 4 Pl. Jussieu, 75252 Paris, France

The contribution of the box and crossed two-pion-exchange diagrams to proton-proton scattering at  $90^\circ_{c.m.}$  is calculated in the laboratory momentum range up to 12 GeV/c. Relativistic form factors related to the nucleon and pion size and representing the pion source distribution based on the quark structure of the hadronic core are included at each vertex of the pion-nucleon interaction. These form factors depend on the four-momenta of the exchanged pions and scattering nucleons. Feynman-diagram amplitudes calculated without form factors are checked against those derived from dispersion relations. In this comparison, one notices that a very short-range part of the crossed diagram, neglected in dispersion-relation calculations of the two-pion-exchange nucleon-nucleon potential, gives a sizable contribution. In the Feynman-diagram calculation with form factors the agreement with measured spin-separated cross sections, as well as amplitudes in the lower part of the energy range considered, is much better for pion-nucleon pseudo-vector vis à vis pseudo-scalar coupling. While strengths of the box and crossed diagrams are comparable for laboratory momenta below 2 GeV/c, the crossed diagram dominates for larger momenta, largely due to the kinematics of the crossed diagram allowing a smaller momentum transfer in the nucleon center of mass. An important contribution arises from the principal-value part of the integrals which is non-zero when form factors are included. It seems that the importance of the exchange of color singlets may extend higher in energy than expected.

## I. INTRODUCTION

The nucleon-nucleon interaction at intermediate energy (up to 12 GeV/c laboratory momentum,  $P_{Lab}$ ) has been the focus of a number of experimental [1, 2, 3, 4, 5, 6, 7, 8, 9] and theoretical [10, 11, 12, 13] studies. The momentum dependence of the spin transfer shows a very interesting behavior. The spin correlation observable,  $C_{NN}$ , for proton-proton scattering at  $90^\circ_{c.m.}$ , has values near unity at low energies, decreases to a constant value of around 0.07 from 4 GeV/c to 8 GeV/c and then increases to values around 0.5.

While one-pion exchange has been shown to be a very important contributor to the NN interaction at low energies [14, 15, 16] and at higher energies at small momentum transfer [17], it alone predicts a constant value of 1/3 for  $C_{NN}$ . Not only is this value in disagreement with the data, but it is not expected that single pion exchange will still be important at this higher momentum transfer (see Fig. 1 and comments below).

Brodsky [10] and Farrar [11] have shown that the simple quark-exchange mechanism also gives 1/3 for  $C_{NN}$ . No calculations of absolute cross sections with quark-exchange models exist to our knowledge, although predictions do exist [18] for the energy dependence of the cross section. These predictions for the slope are in quite good agreement, not only with proton-proton scattering, but with other scattering processes at high energies.

While it is natural to think that this behavior could be an indicator of the nature of the elastic scattering process, this idea of the identification of a mechanism has languished for many years for lack of candidate theories. We present here the calculation of the contribution of two-pion exchange in this energy region. We find that this mechanism predicts the right size for the cross section, hence provides a candidate theory for the dominant mechanism in this intermediate energy region.

The interest in two-pion exchange as a contributor to the nucleon-nucleon interaction is very old, beginning just after the discovery of the pion [19, 20, 21, 22, 23]. The seminal work of Partovi and Lomon [24] was one of the first to create a viable potential based on this idea. Since these works were aimed at obtaining the two-pion-exchange contribution to the NN potential, non-relativistic approximations were made.

The Paris potential group [25, 26, 27] has worked extensively with this contribution within a dispersion relation approach. Again, the interest was primarily to obtain a non-relativistic potential for the nucleon-nucleon interaction.

Studies of the relation of chiral symmetry to the two-pion-exchange potential have been made recently [28, 29] which led to more recent studies by Rentmester et al. [30] on the long range part of the two-pion-exchange potential. Ref. [30] concludes that there is strong evidence for the existence and importance of two-pion exchange.

Seeing this significant body of study at low energy, it is natural to ask about the two-pion interaction at higher energies. We will investigate its role by calculating the lowest order Feynman graphs [31] for this process in the range  $P_{Lab}$  from 0 to 12 GeV/c.

Before beginning the calculations, some discussion is needed as to the general approach. A common methodology has been to proceed by ranges [19, 20]. In this point of view one says that the one- and two-pion exchange are valid (and give essentially all of the potential) beyond a certain inter-nucleon separation. In order to confront the data it is then necessary to construct the potential at shorter ranges, perhaps with phenomenology as in Ref. [26]. We take the point of view that the pion exchanges are between quarks and hence (to some approximation) the interaction calculated remains valid even at short distances. There is no reason *a priori* to exclude pion exchange at short distances provided that the distribution of quarks within the nucleon is properly taken into account. Even when the relative coordinate between the *centers* is zero the range of the exchange between the quarks will be of the order of the size of the nucleon. In fact, there are a number of studies [32] of baryon spectra based on the exchange of mesons between quarks within the interior of a single nucleon.

Of course, we do not expect that one- and two-pion exchanges represent the entire interaction, other contributions are certainly present. We calculate the two-pion contribution with a view to examining to what extent the scattering properties can be explained with this mechanism alone.

Since a common view is that nucleons and pions have an intrinsic finite size, the present approach includes the form factor resulting from this distribution in the Feynman integrals. There is a long history of treating form factors of complex systems in nuclear physics. It is often regarded as the amplitude for the probability of being able to transfer the three-momentum represented by its argument to the object while leaving it intact, hence is related to the probability of an *elastic* scattering or absorption.

The inclusion of such a form factor is not simple, however. The full Feynman integrals are in four dimensions, requiring a form factor with a dependence on all 4 variables. Many form factors deal only with three-momentum, although the problem of adding a fourth variable has been addressed by a number of groups (see section IV for a discussion). We approach the problem of the form factor from the point of view of invariants and analyticity with

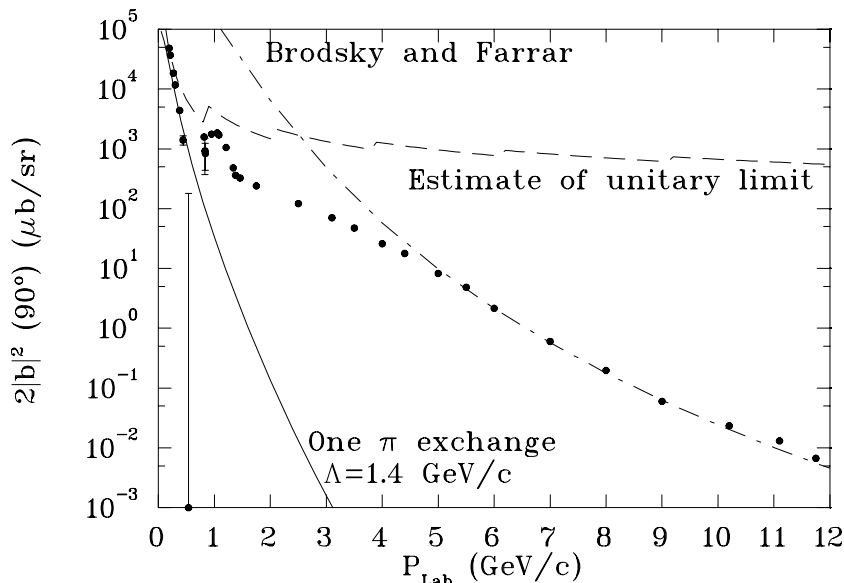


FIG. 1: Values of  $2|b|^2$  (see Ref. [36] and appendix A) at  $90^\circ_{c.m.}$ , extracted as discussed in the text, compared with one-pion exchange and an estimated unitary limit. The dash-dot curve gives the energy dependence predicted by Brodsky and Farrar [18] normalized at 6 GeV/c.

guidance from the argument that the function should represent a boost into the center of mass frame of the nucleon in the on-shell limit. We will argue that a selection can be made on this dependence according to the view of the physical origin of the size of the system, i.e. if it arises from the interaction with virtual mesons (or more generally the sea) or with the “permanent” quark core constituents. We assume here that the pion exchanges take place between quarks contained within the core of the nucleon.

We will treat the cases of both pure pseudo-scalar (PS) and pure pseudo-vector (PV) coupling even though some authors have found evidence for a mixture of the couplings [33, 34, 35]. Some of the integrals involved in the PV calculation are divergent and, while the PS integrals converge, the resulting cross sections are orders of magnitude too large at the higher energies if no form factor is included. The introduction of form factors solves divergence problems which arise in the calculation but, more importantly, it takes into account the confinement core of the nucleon explicitly introducing an interaction range of this size.

To represent the proton-proton amplitude, we use the Saclay [36] decomposition into components called  $a$ ,  $b$ ,  $c$ ,  $d$  and  $e$ . These independent amplitudes have individual characteristics similar to common non-relativistic representations (see appendix A in Ref. [17]) and hence provide a natural extension of our familiar concepts of the spin dependence of the amplitude at low energy. At  $90^\circ$  center of mass scattering angle, some simplification occurs since  $a \equiv 0$  and  $b \equiv -c$  so that only 3 independent amplitudes are needed.

For data comparison we combine the values of  $C_{NN}$  [1, 2, 3] with the measured cross sections at  $90^\circ$  [7, 8, 9] to obtain the value of the absolute square of the Saclay  $b$  amplitude and the sum of the absolute squares of the  $d$  and  $e$  amplitudes (see Appendix A). These experimental measurements will constitute the primary data with which we will compare. Figure 1 shows the values of  $2|b|^2$  compared with a calculation of the corresponding values from one-pion exchange with a dipole form factor with a range of  $\Lambda = 1.4$  GeV/c (see Section IV for a discussion of this quantity). The one-pion-exchange mechanism is clearly important below 1 GeV/c but the predicted cross section decreases rapidly above that.

There are other problems with the comparison with data of a simple perturbative calculation of the type that we make here. The results will not, in general, be unitary. At low energies it is not reasonable to compare with data without a unitary theory, which is the reason that a potential is normally calculated and followed by a solution of the Schrödinger equation or a relativistic generalization. We have made an estimate of what might be expected for a maximum cross section at  $90^\circ$  based on unitarity by setting each partial-wave S-matrix element to  $-1$  and performing the partial-wave sum up to  $k_{c.m.}R$  where  $R$  was taken as 1 fm. From this estimate we see that above about 1.5 GeV/c

the experimental cross section is sufficiently below this limit that unitarity can be expected to play a minor role. The introduction of a form factor also leads to questions about causality [37, 38, 39] which we discuss in section IV.

Section II gives the general method of calculation with the introduction of the pseudo-scalar and pseudo-vector operators for the box and crossed kinematics. Section III develops the method for the numerical treatment of the singularities of the propagators. Section IV introduces the form factors used and discusses their physical basis. Section V presents the dispersion relation calculation. Section VI gives the basic results of the study while section VII gives a summary of the work and states some conclusions. Appendix A gives the projection of the spin-dependent amplitudes onto the Saclay amplitudes, appendix B outlines the general method used to treat the singularities numerically and appendix C gives an interpretation of the variable used in the form factor in terms of a four-dimensional cross product.

## II. METHOD OF CALCULATION

The differential cross section in the center of mass (c.m.) is written in terms of the matrix element,  $\mathcal{M}$ , as

$$\sigma(\theta) = \left( \frac{m^2}{4\pi E} \right)^2 |\mathcal{M}|^2. \quad (1)$$

Here  $E$  is the energy of one proton in the c.m. and  $m$  is the proton mass. Spin sums are implicit. Since we consider both the box and crossed diagrams,  $\mathcal{M}$  will be the sum of the two. We will study only the cases of pure pseudo-scalar or pure pseudo-vector coupling.

### A. Pseudo-scalar Coupling

#### 1. Box Diagram

We may write the Feynman diagram for the matrix element with the box kinematics (see Fig. 2) as

$$\begin{aligned} \mathcal{M}_{PS} \delta(k_1 + k_2 - k'_1 - k'_2) = \\ \frac{g^4}{(2\pi)^4} \int \frac{dq dq' dp dp'}{(p^2 - m^2 + i\epsilon)(p'^2 - m^2 + i\epsilon)(q^2 - \mu^2 + i\epsilon)(q'^2 - \mu^2 + i\epsilon)} \mathcal{F}(k_1, k_2, k'_1, k'_2, q, q') \\ \times \delta(q - p + k_1) \delta(q' - p + k'_1) \delta(-q - p' + k_2) \delta(-q' - p' + k'_2). \end{aligned} \quad (2)$$

Here  $g$  is the pseudo-scalar coupling constant with the normalization  $\frac{g^2}{4\pi} = 13.75$  and  $\mathcal{F}(k_1, k_2, k'_1, k'_2, q, q')$  is the form factor derived from the intrinsic size of the interacting system. Since  $\mathcal{F}$  is assumed to have no spin dependence and has no poles on the real axes, it plays no direct role in the treatment of singularities or spin reduction. We suppress the arguments of  $\mathcal{F}$  in the equations for the remainder of this section and for the next section. Using the first and third delta function to eliminate the integral over  $p$  and  $p'$  and the (one dimensional) relationship  $\delta(x)\delta(y) = 2\delta(x+y)\delta(x-y)$ , the remaining two delta functions can be written as

$$2^4 \delta(k_1 + k_2 - k'_1 - k'_2) \delta(2q - 2q' + k_1 - k_2 + k'_2 - k'_1).$$

The first delta function factors out of the integral and cancels the one on the left-hand-side of Eq. (2).

We work in the center-of-mass system where

$$\mathbf{k}_1 = -\mathbf{k}_2 \equiv \mathbf{k}, \quad E_1 = E_2, \quad \mathbf{k}'_1 = -\mathbf{k}'_2 \equiv \mathbf{k}', \quad E'_1 = E'_2, \quad (3)$$

since the external lines are on shell and

$$E_1 = E'_2 \equiv E \quad (4)$$

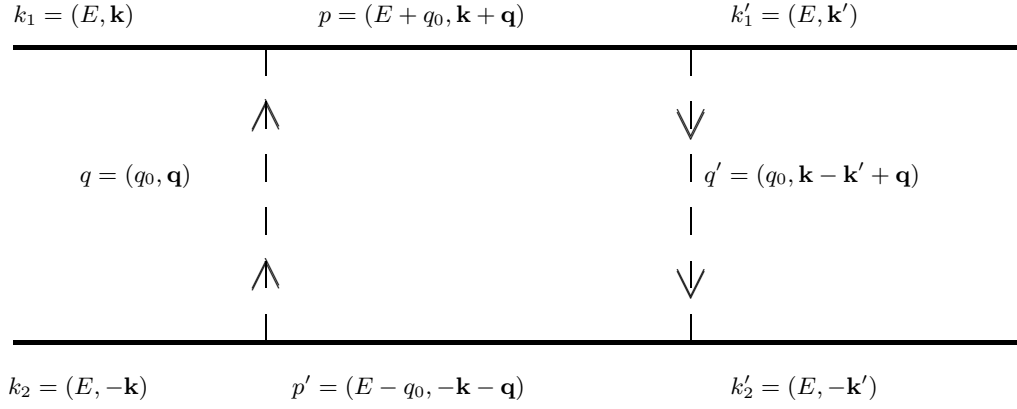


FIG. 2: Kinematics for the box diagram. Note that in our calculation, starting from Eq. (2) form factors are used at each vertex even though we have not indicated their presence here.

by the conservation of energy. With these relations, the remaining delta function under the integral sign becomes

$$2^4 \delta(2q - 2q' + 2k - 2k') = \delta(q - q' + k - k').$$

For the box, (see Fig. 2), we have

$$\mathbf{p} = \mathbf{k} + \mathbf{q} = \mathbf{k}' + \mathbf{q}', \quad \mathbf{p}' = -\mathbf{k} - \mathbf{q} = -\mathbf{k}' - \mathbf{q}', \quad \mathbf{p}' = -\mathbf{p}, \quad (5)$$

and

$$q_0 = q'_0; \quad p_0 = E + q_0; \quad p'_0 = E - q_0. \quad (6)$$

Thus, the expression to be evaluated reduces to a 4-dimensional integral

$$\mathcal{M}_{PS} = \frac{g^4}{(2\pi)^4} \int \frac{dq [\bar{u}(E, \mathbf{k}') \gamma_5 (\not{p} + m) \gamma_5 u(E, \mathbf{k})]^1 [\bar{u}(E, -\mathbf{k}') \gamma_5 (\not{p}' + m) \gamma_5 u(E, -\mathbf{k})]^2}{(p^2 - m^2 + i\epsilon)(p'^2 - m^2 + i\epsilon)(q^2 - \mu^2 + i\epsilon)(q'^2 - \mu^2 + i\epsilon)} \mathcal{F}. \quad (7)$$

We can reduce the spinor algebra of the operators on the two lines using the general relationship (for on-shell spinors)

$$\bar{u}(E_{v'}, \mathbf{v}') \gamma_5 u(E_v, \mathbf{v}) = \chi^\dagger \frac{\sqrt{(E_{v'} + m)(E_v + m)}}{2m} \boldsymbol{\sigma} \cdot \left[ \frac{\mathbf{v}}{E_v + m} - \frac{\mathbf{v}'}{E_{v'} + m} \right] \chi, \quad (8)$$

where  $\chi$  is a Pauli spinor and we have used

$$u(E_v, \mathbf{v}) = \sqrt{\frac{E_v + m}{2m}} \left( \frac{1}{E_v + m} \right) \chi. \quad (9)$$

Here  $E_v = \sqrt{\mathbf{v}^2 + m^2}$  and  $\boldsymbol{\sigma}$  is the Pauli matrix.

The expression can be written as an operator in spin space in the form

$$\mathcal{M}_{PS} = \frac{g^4}{(2\pi)^4} \int \frac{dq \Theta_1(p_0, \mathbf{p}) \Theta_2(p'_0, \mathbf{p}') \mathcal{F}}{(p^2 - m^2 + i\epsilon)(p'^2 - m^2 + i\epsilon)(q^2 - \mu^2 + i\epsilon)(q'^2 - \mu^2 + i\epsilon)}. \quad (10)$$

With

$$\bar{u}_{r'}(E, \mathbf{k}') \gamma_5 (\not{p} + m) \gamma_5 u_r(E, \mathbf{k}) = \bar{u}_{r'}(E, \mathbf{k}') (-\gamma_0 p_0 + m + \boldsymbol{\gamma} \cdot \mathbf{p}) u_r(E, \mathbf{k}), \quad (11)$$

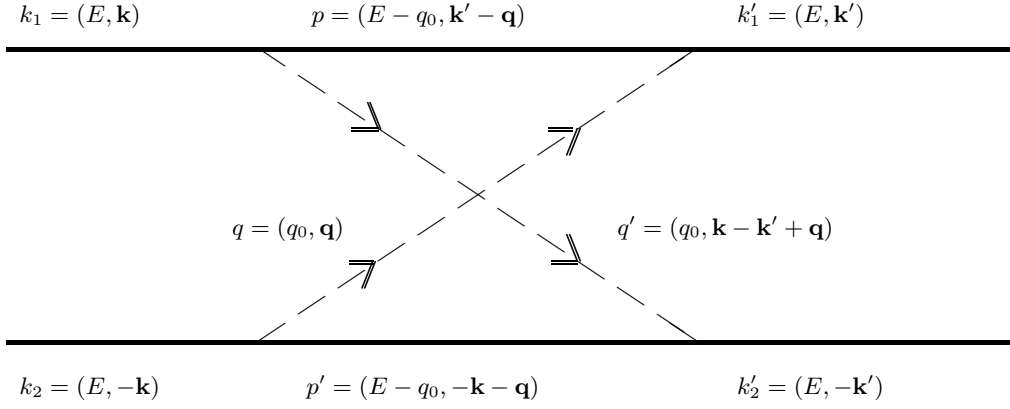


FIG. 3: Crossed diagram kinematics. Form factors are to be included here as in Fig. 2.

$\Theta_1$  can be written as an operator between Pauli spinors  $\chi_{r'}$  and  $\chi_r$  where the index  $r$  corresponds to the spin of the proton,

$$\begin{aligned}
2m\Theta_1 &= -p_0(E+m) \left( 1 + \frac{\boldsymbol{\sigma}_1 \cdot \mathbf{k}' \boldsymbol{\sigma}_1 \cdot \mathbf{k}}{(E+m)^2} \right) + m(E+m) \left( 1 - \frac{\boldsymbol{\sigma}_1 \cdot \mathbf{k}' \boldsymbol{\sigma}_1 \cdot \mathbf{k}}{(E+m)^2} \right) \\
&\quad + (E+m) \left( 1 - \frac{\boldsymbol{\sigma}_1 \cdot \mathbf{k}'}{E+m} \right) \begin{pmatrix} 0 & \boldsymbol{\sigma}_1 \cdot \mathbf{p} \\ -\boldsymbol{\sigma}_1 \cdot \mathbf{p} & 0 \end{pmatrix} \begin{pmatrix} 1 \\ \frac{\boldsymbol{\sigma}_1 \cdot \mathbf{k}}{E+m} \end{pmatrix}, \\
2m\Theta_1 &= E^+(m-p_0) - \frac{\boldsymbol{\sigma}_1 \cdot \mathbf{k}' \boldsymbol{\sigma}_1 \cdot \mathbf{k}}{E^+} (m+p_0) + \boldsymbol{\sigma}_1 \cdot \mathbf{p} \boldsymbol{\sigma}_1 \cdot \mathbf{k} + \boldsymbol{\sigma}_1 \cdot \mathbf{k}' \boldsymbol{\sigma}_1 \cdot \mathbf{p},
\end{aligned}$$

$$2m\Theta_1 = E^+(m-p_0) - \frac{m+p_0}{E^+} (\mathbf{k} \cdot \mathbf{k}' + i\boldsymbol{\sigma}_1 \cdot \mathbf{k}' \times \mathbf{k}) + \mathbf{p} \cdot (\mathbf{k} + \mathbf{k}') + i\boldsymbol{\sigma}_1 \cdot \mathbf{p} \times (\mathbf{k} - \mathbf{k}'), \quad (12)$$

where  $E^+ = E + m$ . These expressions allow us to identify  $G$  and  $\mathbf{H}$  in the operator,

$$2m\Theta_1 = G + i\boldsymbol{\sigma}_1 \cdot \mathbf{H}, \quad (13)$$

$$G = E^+(m-p_0) - \frac{m+p_0}{E^+} \mathbf{k} \cdot \mathbf{k}' + \mathbf{p} \cdot (\mathbf{k} + \mathbf{k}'), \quad (14)$$

$$\mathbf{H} = - \left[ \frac{m+p_0}{E^+} \mathbf{k}' \times \mathbf{k} - \mathbf{p} \times (\mathbf{k} - \mathbf{k}') \right]. \quad (15)$$

For the lower line where

$$2m\Theta_2 = G' + i\boldsymbol{\sigma}_2 \cdot \mathbf{H}', \quad (16)$$

$$G' = E^+(m-p'_0) - \frac{m+p'_0}{E^+} \mathbf{k} \cdot \mathbf{k}' - \mathbf{p}' \cdot (\mathbf{k} + \mathbf{k}'); \quad \mathbf{H}' = - \left[ \frac{m+p'_0}{E^+} \mathbf{k}' \times \mathbf{k} + \mathbf{p}' \times (\mathbf{k} - \mathbf{k}') \right]. \quad (17)$$

## 2. Crossed Diagram

The expressions for the matrix element in Eq. (10), and for  $\Theta_1$  and  $\Theta_2$ , for the two-pion crossed diagram are the same as in the case of the box except that now the relations between momenta are those corresponding to the diagram in Fig. 3,

$$\mathbf{p} + \mathbf{q}' = \mathbf{k}, \quad \mathbf{p}' + \mathbf{q} = -\mathbf{k}, \quad \mathbf{p} + \mathbf{q} = \mathbf{k}', \quad \mathbf{p}' + \mathbf{q}' = -\mathbf{k}', \quad (18)$$

$$p_0 = p'_0; \quad q_0 = q'_0; \quad q_0 = E - p_0. \quad (19)$$

Since only neutral pions can be exchanged in the case of the box diagram and both neutral and charged pions can be exchanged in the crossed diagram, a factor of 5 multiplies the crossed diagram result. This isospin factor is explicitly given in the dispersion relation approach in Eqs. (169) and (170).

## B. Pseudo-vector Coupling

In this case the interaction is given by  $\frac{f}{\mu} \bar{\psi} \gamma_\mu \gamma_5 \tau \cdot \partial^\mu \phi_\pi \psi$  and for one nucleon propagator,  $P_{PV}$ , the expectation value leads to

$$P_{PV}(p^2 - m^2 + i\epsilon) = -\frac{f^2}{\mu^2} \bar{u}(k') \not{q}' \gamma_5 (\not{p} + m) \not{q} \gamma_5 u(k). \quad (20)$$

Using  $k + q = p = k' + q'$  and the Dirac equation  $(\not{k} - m)u(k) = 0$  we can write

$$P_{PV}(p^2 - m^2 + i\epsilon) = \frac{f^2}{\mu^2} \bar{u}(k') \gamma_5 (\not{p} + m) (\not{p} + m) (\not{p} + m) \gamma_5 u(k). \quad (21)$$

By regrouping the terms

$$P_{PV}(p^2 - m^2 + i\epsilon) = \frac{f^2}{\mu^2} \bar{u}(k') \gamma_5 (\not{p} + m) [(\not{p} - m) + 2m] [(\not{p} - m) + 2m] \gamma_5 u(k), \quad (22)$$

we find

$$P_{PV}(p^2 - m^2 + i\epsilon) = \frac{f^2}{\mu^2} \bar{u}(k') \gamma_5 (p^2 - m^2) (\not{p} + 3m) \gamma_5 u(k) + \frac{f^2 4m^2}{\mu^2} \bar{u}(k') \gamma_5 (\not{p} + m) \gamma_5 u(k). \quad (23)$$

The last term can be seen to be the pseudo-scalar expression considered in the last section for one nucleon propagator. Hence, the operator can be separated into a term which corresponds to a contact term and one which is identical to the pseudo-scalar expression developed before.

$$P_{PV} = \frac{f^2}{\mu^2} \bar{u}(k') \gamma_5 (\not{p} + 3m) \gamma_5 u(k) + g^2 \frac{\bar{u}(k') \gamma_5 (\not{p} + m) \gamma_5 u(k)}{p^2 - m^2} \equiv P_C + P_{PS}, \quad (24)$$

where we have used the standard correspondence  $g^2 = \frac{f^2 4m^2}{\mu^2}$ . We can write

$$P_C = \frac{g^2}{4m^2} \left[ 2m \bar{u}_{r'}(k') u_r(k) + \chi_{r'}^\dagger \Theta_1(p_0, \mathbf{p}) \chi_r \right]. \quad (25)$$

It is useful to define an operator analogous to the  $\Theta_1(p_0, \mathbf{p})$  as before for the contact term for the upper line for the case of the box diagram

$$\chi_{r'}^\dagger C_1(p_0, \mathbf{p}) \chi_r = 2m \bar{u}_{r'}(k') u_r(k) + \chi_{r'}^\dagger \Theta_1(p_0, \mathbf{p}) \chi_r. \quad (26)$$

We can also define operators corresponding to the contact terms which are very similar to those defined before in Eqs. (14) and (15).

$$G_C = G + 2m \left( E^+ - \frac{\mathbf{k}' \cdot \mathbf{k}}{E^+} \right); \quad G'_C = G' + 2m \left( E^+ - \frac{\mathbf{k}' \cdot \mathbf{k}}{E^+} \right), \quad (27)$$

$$\mathbf{H}_C = \mathbf{H} - 2m \frac{\mathbf{k}' \times \mathbf{k}}{E^+}; \quad \mathbf{H}'_C = \mathbf{H}' - 2m \frac{\mathbf{k}' \times \mathbf{k}}{E^+}, \quad (28)$$

with

$$2mC_1(p_0, \mathbf{p}) = G_C + i\boldsymbol{\sigma}_1 \cdot \mathbf{H}_C; \quad 2mC_2(p_0, \mathbf{p}) = G'_C + i\boldsymbol{\sigma}_2 \cdot \mathbf{H}'_C. \quad (29)$$

The same generalization to the crossed diagram can be made as in the previous section and we do not repeat it here. We can write for either the box or crossed diagram

$$\begin{aligned} \mathcal{M}_{PV} = & \frac{g^4}{16m^4} \frac{1}{(2\pi)^4} \int dq \frac{C_1(p_0, \mathbf{p})C_2(p'_0, \mathbf{p}')\mathcal{F}}{(q_0^2 - \omega^2)(q_0^2 - \omega'^2)} + \frac{g^4}{4m^2} \frac{1}{(2\pi)^4} \int dq \frac{C_1(p_0, \mathbf{p})\Theta_2(p'_0, \mathbf{p}')\mathcal{F}}{(p'^2 - m^2)(q_0^2 - \omega^2)(q_0^2 - \omega'^2)} \\ & + \frac{g^4}{4m^2} \frac{1}{(2\pi)^4} \int dq \frac{\Theta_1(p_0, \mathbf{p})C_2(p'_0, \mathbf{p}')\mathcal{F}}{(p^2 - m^2)(q_0^2 - \omega^2)(q_0^2 - \omega'^2)} + \mathcal{M}_{PS}. \end{aligned} \quad (30)$$

The first term will be referred to as the bubble diagram and the second and third (numerically equal) as the triangle.

### III. TREATMENT OF SINGULARITIES

In principle, each of the propagators contribute two  $\delta$ -functions and two principal-value integrals. However, for one fermion on shell neither pion can be on shell and for one pion on shell neither fermion can be on shell. This fact considerably reduces the number of terms which contribute. For numerical calculation, the poles and their order must be identified and separated into  $\delta$ -function and principal value parts. The general technique for doing this is outlined in Appendix B. We cannot use the classical methods of reduction [31] because of the existence of the form factor at each vertex. In the following we treat the case for a general scattering angle  $\chi$  and assume that the incident beam direction, parallel to  $\mathbf{k}$ , is along the z-axis and the final proton momentum,  $\mathbf{k}'$ , lies in the z-x plane.

#### A. Contact-Contact Term (Bubble Diagram)

For the first term in Eq. (30) for either the crossed or box configuration we have

$$\mathcal{M}_{CC} = \frac{g^4}{16m^4} \frac{1}{(2\pi)^4} \int d\mathbf{q} \int_{-\infty}^{\infty} dq_0 \frac{C_1(p_0, \mathbf{p})C_2(p'_0, \mathbf{p}')\mathcal{F}}{(q_0^2 - \omega^2 + i\epsilon)(q_0^2 - \omega'^2 + i\epsilon)} \quad (31)$$

$$= \frac{g^4}{16m^4} \frac{1}{(2\pi)^4} \int d\Omega \int_0^{\infty} d\tilde{q} \int_{-\infty}^{\infty} dq_0 \frac{O(q_0, \mathbf{q})\mathcal{F}}{(q_0^2 - \omega^2 + i\epsilon)(q_0^2 - \omega'^2 + i\epsilon)}, \quad (32)$$

where  $\tilde{q} = |\mathbf{q}|$  and the volume factor  $\tilde{q}^2$  has been included in  $O(q_0, \mathbf{q})$ . Taking large finite limits for the integrals

$$\mathcal{M}_{CC} = -\frac{g^4}{16m^4} \frac{1}{(2\pi)^4} \int d\Omega \int_0^{\tilde{q}_{max}} \frac{d\tilde{q}}{\omega^2 - \omega'^2} \int_{-q_0^{max}}^{q_0^{max}} dq_0 O(q_0, \mathbf{q}) \left[ \frac{1}{q_0^2 - \omega^2 + i\epsilon} - \frac{1}{q_0^2 - \omega'^2 + i\epsilon} \right] \mathcal{F}. \quad (33)$$



If we consider the contribution of one pole in  $q_0$  ( $q_0 = \omega$  for example) then a counting of powers of  $\tilde{q}$  in the numerator and denominator shows that, for large  $\tilde{q}$ , the integrand is proportional to  $\tilde{q}$  so that the integral diverges as  $\tilde{q}_{max}^2$  if the form factor is set to a constant. The integral can now be evaluated by the method given in Appendix B.

For the first term of the integrand of the solid angle we have

$$\int_0^{\tilde{q}_{max}} \frac{d\tilde{q}}{\omega^2 - \omega'^2 + i\epsilon} \int_{-q_0^{max}}^{q_0^{max}} dq_0 \frac{O(q_0, \mathbf{q}) \mathcal{F}}{q_0^2 - \omega^2 + i\epsilon} \quad (34)$$

$$= \int_0^{\tilde{q}_{max}} \frac{d\tilde{q}}{\omega^2 - \omega'^2 + i\epsilon} \int_{-q_0^{max}}^{q_0^{max}} dq_0 \left[ \frac{O(q_0, \mathbf{q}) - T(q_0, \mathbf{q})}{q_0^2 - \omega^2 + i\epsilon} + \frac{T(q_0, \mathbf{q})}{q_0^2 - \omega^2 + i\epsilon} \right] \mathcal{F} = \int_0^{\tilde{q}_{max}} \frac{d\tilde{q}}{\omega^2 - \omega'^2 + i\epsilon} F(\tilde{q}, \Omega), \quad (35)$$

where

$$F(\tilde{q}, \Omega) = \int_{-q_0^{max}}^{q_0^{max}} dq_0 \frac{O(q_0, \mathbf{q}) - T(q_0, \mathbf{q})}{q_0^2 - \omega^2} \mathcal{F} \\ + \mathcal{F} \frac{[O(\omega, \mathbf{q}) + O(-\omega, \mathbf{q})]}{2\omega} \ln \frac{q_0^{max} - \omega}{q_0^{max} + \omega} - \frac{i\pi}{2\omega} [O(\omega, \mathbf{q}) + O(-\omega, \mathbf{q})] \mathcal{F} \quad (36)$$

and

$$T(q_0, \mathbf{q}) = \left[ \frac{q_0 + \omega}{2\omega} O(\omega, \mathbf{q}) - \frac{q_0 - \omega}{2\omega} O(-\omega, \mathbf{q}) \right] \mathcal{F}. \quad (37)$$

We have included the  $+i\epsilon$  in the denominator of the external factor  $1/(\omega^2 - \omega'^2)$  but, in fact, there is no singularity in the combined integral so this choice is arbitrary. The remaining indicated integral is computed numerically. We now need to treat the singularity in the  $\tilde{q}$  integral in a similar manner. Since

$$\omega^2 - \omega'^2 = \mathbf{q}^2 - \mathbf{q}'^2 = -2k^2(1 - \cos \chi) - 2\mathbf{q} \cdot (\mathbf{k} - \mathbf{k}') = -2kX(\tilde{q} - w) \quad (38)$$

with

$$X = x(1 - \cos \chi) - \sqrt{1 - x^2} \sin \chi \cos \phi \xrightarrow{\chi=90^\circ} \cos \theta - \sin \theta \cos \phi; \quad \text{and} \quad w \equiv -k(1 - \cos \chi)/X. \quad (39)$$

Here  $\theta$  and  $\phi$  are the angles of  $\mathbf{q}$  in polar coordinates and  $x = \cos \theta$ . We can now write

$$\int_0^{\tilde{q}_{max}} \frac{d\tilde{q}}{\omega^2 - \omega'^2 + i\epsilon} F(\tilde{q}, \Omega) = -\frac{1}{2kX} \int_0^{\tilde{q}_{max}} \frac{d\tilde{q} F(\tilde{q}, \Omega)}{\tilde{q} - w + i\epsilon} \quad (40)$$

$$= -\frac{1}{2kX} \int_0^{\tilde{q}_{max}} \frac{d\tilde{q} [F(\tilde{q}, \Omega) - F(w, \Omega)]}{\tilde{q} - w} - \frac{1}{2kX} \ln(\tilde{q}_{max}/w - 1) + \frac{i\pi}{2kX} F(w, \Omega). \quad (41)$$

The imaginary parts will cancel when the two terms of Eq. (33) are combined.

## B. Contact-PS and PS-Contact Terms (Triangle Diagram)

In this case there is one nucleon propagator in addition to the two pion propagator and the second and third terms in Eq. (30) can be written in the form

$$-\frac{g^4}{4m^2} \frac{1}{(2\pi)^4} \int d\Omega \int_0^{\tilde{q}_{max}} \frac{d\tilde{q}}{\omega^2 - \omega'^2 + i\epsilon} \int_{-q_0^{max}}^{q_0^{max}} dq_0 \frac{O(q_0, \mathbf{q})}{p_0^2 - E_p^2 + i\epsilon} \left[ \frac{1}{q_0^2 - \omega^2 + i\epsilon} - \frac{1}{q_0^2 - \omega'^2 + i\epsilon} \right] \mathcal{F}. \quad (42)$$

A count of the powers of  $\tilde{q}$  at a pole of  $q_0$  shows that the integrand varies as  $1/\tilde{q}$  for large  $\tilde{q}$  so the integral diverges (in the absence of a form factor) logarithmically in  $\tilde{q}_{max}$ . Again there are no double poles and the first method of Appendix B can be used to calculate the 4 poles in  $q_0$ .

For the crossed-pion configuration we define, for the first term in the above equation

$$P_1 = E - E_p; \quad P_2 = E + E_p; \quad P_3 = \omega; \quad P_4 = -\omega, \quad (43)$$

while for the second we have,

$$P_1 = E - E_p; \quad P_2 = E + E_p; \quad P_3 = \omega'; \quad P_4 = -\omega'. \quad (44)$$

With the definition

$$G(q_0, \mathbf{q}) = \sum_{i=1}^4 \frac{\prod_{j \neq i} (q_0 - P_j)}{\prod_{j \neq i} (P_i - P_j)} O(P_i, \mathbf{q}) \mathcal{F} \quad (45)$$

the integral can be written as

$$-\frac{g^4}{4m^2} \frac{1}{(2\pi)^4} \int d\Omega \int_0^{\tilde{q}_{max}} \frac{d\tilde{q}}{\omega^2 - \omega'^2 + i\epsilon} \left\{ \int_{-q_0^{max}}^{q_0^{max}} dq_0 \left[ \frac{[O(q_0, \mathbf{q}) - G(q_0, \mathbf{q})]}{\prod_{i=1}^4 (q_0 - P_i + i\epsilon)} + \frac{G(q_0, \mathbf{q})}{\prod_{i=1}^4 (q_0 - P_i + i\epsilon)} \right] \mathcal{F} \right\}. \quad (46)$$

The last integral in the above becomes

$$\int_{-q_0^{max}}^{q_0^{max}} dq_0 \frac{G(q_0, \mathbf{q}) \mathcal{F}}{\prod_{i=1}^4 (q_0 - P_i + i\epsilon)} = \sum_{i=1}^4 \int_{-q_0^{max}}^{q_0^{max}} dq_0 \frac{O(P_i, \mathbf{q}) \mathcal{F}}{(q_0 - P_i + i\epsilon) \prod_{j \neq i} (P_i - P_j)} \quad (47)$$

$$= \sum_{i=1}^4 \frac{O(P_i, \mathbf{q}) \mathcal{F}}{\prod_{j \neq i} (P_i - P_j)} \ln \left( \frac{q_0^{max} - P_i}{q_0^{max} + P_i} \right) + i\pi \sum_{i=1}^4 \frac{O(P_i, \mathbf{q}) \mathcal{F}}{\prod_{j \neq i} (P_i - P_j)}. \quad (48)$$

### C. PS-PS Term

The pseudo-scalar term is given by Eq. (10). There are now two more factors of  $\tilde{q}$  in the denominator so the integral is convergent. For this case, i.e. when there are two nucleon poles, the box and crossed diagrams must be treated separately.

#### 1. Crossed Diagram

For the crossed-pion configuration, where  $p_0 = p'_0 = E - q_0$ , there is formally a second order pole when  $E_p = E_{p'}$ , so we write

$$\begin{aligned} & \frac{1}{(p_0^2 - E_p^2 + i\epsilon)(p_0^2 - E_{p'}^2 + i\epsilon)(q_0^2 - \omega^2 + i\epsilon)(q_0^2 - \omega'^2 + i\epsilon)} \\ &= \frac{1}{E_p^2 - E_{p'}^2} \left[ \frac{1}{p_0^2 - E_p^2 + i\epsilon} - \frac{1}{p_0^2 - E_{p'}^2 + i\epsilon} \right] \frac{1}{\omega^2 - \omega'^2} \left[ \frac{1}{q_0^2 - \omega^2 + i\epsilon} - \frac{1}{q_0^2 - \omega'^2 + i\epsilon} \right]. \end{aligned} \quad (49)$$

The integration can now be done with the methods of Appendix B with four poles in the  $q_0$  integration.

The first factor can be evaluated using

$$E_p^2 - E_{p'}^2 = \mathbf{p}^2 - \mathbf{p}'^2 = (\mathbf{k}' - \mathbf{q})^2 - (\mathbf{q} + \mathbf{k})^2 = -2\tilde{q}|\mathbf{k}|f(x), \quad (50)$$

where

$$f(x) = x(1 + \cos \chi) + \sqrt{1 - x^2} \cos \phi \sin \chi \xrightarrow{\chi=90^\circ} (x + \sqrt{1 - x^2} \cos \phi). \quad (51)$$

From this expression we see that the second pole has been transformed to the  $x$  integration. The singularity falls at

$$x_0 = -\frac{\sin \chi \cos \phi}{\sqrt{(1 + \cos \chi)^2 + \sin^2 \chi \cos^2 \phi}} \xrightarrow{\chi=90^\circ} -\frac{\cos \phi}{\sqrt{1 + \cos^2 \phi}} \quad (52)$$

and gives a delta-function contribution of the type  $\delta[f(x)]$  with

$$f'(x_0) = 1 + \cos \chi + \frac{\sin^2 \chi \cos^2 \phi}{1 + \cos \chi} \xrightarrow{\chi=90^\circ} 1 + \cos^2 \phi. \quad (53)$$

Thus, for the first of the four terms in Eq. (49) we can write

$$-\frac{g^4}{2k(2\pi)^4} \int d\phi \int_{-1}^1 \frac{dx}{f(x)} \int_0^{\tilde{q}_{max}} \frac{d\tilde{q}}{\tilde{q}(\omega^2 - \omega'^2)} \int_{-q_0^{max}}^{q_0^{max}} \frac{dq_0 O(q_0, \mathbf{q}) \mathcal{F}}{(p_0^2 - E_p^2 + i\epsilon)(q_0^2 - \omega^2 + i\epsilon)} \quad (54)$$

$$= -\frac{g^4}{2k(2\pi)^4} \int d\phi \int_{-1}^1 dx \frac{J(x, \phi)}{f(x) + i\epsilon} \quad (55)$$

$$= -\frac{g^4}{2k(2\pi)^4} \int d\phi \int_{-1}^1 dx \left[ \frac{J(x, \phi) - Q(x, \phi)}{f(x) + i\epsilon} + \frac{Q(x, \phi)}{f(x) + i\epsilon} \right], \quad (56)$$

where

$$Q(x, \phi) \equiv \frac{f(x)}{f'(x_0)(x - x_0 + i\epsilon)} J(x_0, \phi). \quad (57)$$

The first integral in Eq. (56) now has no singularity and can be performed numerically. The second becomes

$$\int_{-1}^1 dx \frac{Q(x, \phi)}{f(x) + i\epsilon} = \frac{J(x_0, \phi)}{f'(x_0)} \int_{-1}^1 \frac{dx}{x - x_0 + i\epsilon} = \frac{J(x_0, \phi)}{f'(x_0)} \ln \left( \frac{1 - x_0}{1 + x_0} \right) - i\pi \frac{J(x_0, \phi)}{f'(x_0)}. \quad (58)$$

## 2. Box Diagram

For the box diagram we have for the pole structure

$$\frac{1}{(p_0^2 - E_p^2 + i\epsilon)(p_0'^2 - E_p^2 + i\epsilon)(q_0^2 - \omega^2 + i\epsilon)(q_0'^2 - \omega'^2 + i\epsilon)}.$$

The pion pole part can be expanded as before but the nucleon poles have a very different development since the fourth integration variable is not the same in the two factors but  $E_p = E_{p'}$  leading to a second order pole. We can write (with  $p_0 = E + q_0$  and  $p_0' = E - q_0$ )

$$\begin{aligned} \frac{1}{[p_0^2 - (E_p - i\epsilon)^2][p_0'^2 - (E_p - i\epsilon)^2]} &= \frac{1}{[(E + q_0)^2 - (E_p - i\epsilon)^2][(E - q_0)^2 - (E_p - i\epsilon)^2]} \\ &= \frac{1}{[q_0^2 - (E + E_p - i\epsilon)^2][q_0'^2 - (E - E_p + i\epsilon)^2]}. \end{aligned} \quad (59)$$

The first factor can be handled by standard methods since there is no second order pole. The second factor, however, does contain a second order pole when  $E_p = E$ . For this factor we write

$$\frac{1}{q_0^2 - (E - E_p + i\epsilon)^2} = \frac{E + E_p}{2(E^2 - E_p^2 + i\epsilon)} \left[ \frac{1}{q_0 - E + E_p - i\epsilon} - \frac{1}{q_0 + E - E_p + i\epsilon} \right].$$

The integral can now be done with the methods of Appendix B with five poles in the  $q_0$  integral in the following manner.

We express

$$E^2 - E_p^2 = k^2 - \mathbf{p}^2 = -\tilde{q}^2 - 2k\tilde{q}x = -\tilde{q}(\tilde{q} + 2kx).$$

Including the pion poles with this factor we have

$$\begin{aligned} & \frac{E + E_p}{2\tilde{q}(\tilde{q} + 2kx + i\epsilon)} \frac{1}{2kX(\tilde{q} - w)} \times \\ & \left[ \frac{1}{q_0 - E + E_p - i\epsilon} - \frac{1}{q_0 + E - E_p + i\epsilon} \right] \left[ \frac{1}{q_0^2 - \omega^2 + i\epsilon} - \frac{1}{q_0^2 - \omega'^2 + i\epsilon} \right], \end{aligned} \quad (60)$$

where  $w$  was defined in Eq. (39).

We expand the factor

$$\frac{1}{(\tilde{q} + 2kx)(\tilde{q} - w)} = \frac{1}{w + 2kx} \left[ \frac{1}{\tilde{q} + 2kx} + \frac{1}{w - \tilde{q}} \right] \quad (61)$$

and write

$$\frac{1}{w + 2kx} = \frac{X}{k(1 - 2xX)} = \frac{X}{kf(x)}, \quad (62)$$

where

$$f(x) = 1 - \cos \chi - 2xc(x) \quad \text{and} \quad c(x) = x - \sin \chi \sqrt{1 - x^2} \cos \phi - x \cos \chi. \quad (63)$$

The function  $f(x)$  has two zeros given by

$$x_{\pm} = \pm \sqrt{\frac{1 \pm \frac{z}{\sqrt{1+z^2}}}{2}} \quad \text{with} \quad z = \frac{\sin \chi \cos \phi}{1 - \cos \chi}. \quad (64)$$

The “+” under the radical goes with the “+” on the exterior and vice versa. The derivatives at the zeros are

$$f'(x_{\pm}) = \frac{2\sqrt{1+z^2}}{x_{\pm}}. \quad (65)$$

Denoting the inner integrals over  $\tilde{q}$  (and  $q_0$ ) as  $J_1$  and  $J_2$  corresponding to the two terms in Eq. (61) we write the integral over the variable  $x$  as

$$-\frac{g^4}{4k^2(2\pi)^4} \int d\phi \int_{-1}^1 dx \left[ \frac{J_1(x, \phi) - Q_i(x, \phi)}{f(x) + i\epsilon} + \frac{Q_i(x, \phi)}{f(x) + i\epsilon} \right], \quad (66)$$

where

$$Q_i(x, \phi) = f(x) \left[ \frac{J_i(x_+, \phi)}{f'(x_+)(x - x_+)} + \frac{J_i(x_-, \phi)}{f'(x_-)(x - x_-)} \right]. \quad (67)$$

The second term in Eq. (66) can be evaluated by

$$\begin{aligned} \int_{-1}^1 dx \frac{Q_i(x, \phi)}{f(x) + i\epsilon} &= \frac{J_i(x_+, \phi)}{f'(x_+)} \ln \left( \frac{1 - x_+}{1 + x_+} \right) - i\pi \frac{J_i(x_+, \phi)}{f'(x_+)} \\ &+ \frac{J_i(x_-, \phi)}{f'(x_-)} \ln \left( \frac{1 - x_-}{1 + x_-} \right) - i\pi \frac{J_i(x_-, \phi)}{f'(x_-)}, \end{aligned} \quad (68)$$

with

$$\begin{aligned} J_1(x, \phi) &= \int_0^\infty d\tilde{q} \tilde{q} \frac{E + E_p}{\tilde{q} + 2kx} \int_{-\infty}^\infty dq_0 \frac{O(q_0, \mathbf{q}) \mathcal{F}}{q_0^2 - (E + E_p - i\epsilon)^2} \times \\ &\left[ \frac{1}{q_0 - E + E_p - i\epsilon} - \frac{1}{q_0 + E - E_p + i\epsilon} \right] \left[ \frac{1}{q_0^2 - \omega^2 + i\epsilon} - \frac{1}{q_0^2 - \omega'^2 + i\epsilon} \right] \end{aligned} \quad (69)$$

and

$$\begin{aligned} J_2(x, \phi) &= \int_0^\infty d\tilde{q} \tilde{q} \frac{E + E_p}{w - \tilde{q}} \int_{-\infty}^\infty dq_0 \frac{O(q_0, \mathbf{q}) \mathcal{F}}{q_0^2 - (E + E_p + i\epsilon)^2} \times \\ &\left[ \frac{1}{q_0 - E + E_p - i\epsilon} - \frac{1}{q_0 + E - E_p + i\epsilon} \right] \left[ \frac{1}{q_0^2 - \omega^2 + i\epsilon} - \frac{1}{q_0^2 - \omega'^2 + i\epsilon} \right]. \end{aligned} \quad (70)$$

#### IV. FORM FACTORS

The two protons are treated as finite-sized particles with their intrinsic internal structure providing an extended source for the exchanged pions. In this case the range of the form factor is not a cut-off parameter to be taken to infinity at the end of the calculation, as is often done in a local field theory, but a physically meaningful quantity. We consider that the true interaction of the pion is with the partons within the nucleons but we use an effective field theory (assumed to obey Feynman rules) to describe the composite system.

##### A. Basic Considerations

In general, one may expect a finite distribution of the interacting constituents of the nucleon to have two components: one due to the confinement range of the valence quarks (and other non-color-singlet partons) and one due to the meson cloud. Because of G parity, the exchange pions cannot couple directly to the pion part of the cloud (likely to be the most important part) and the cloud can be expected to have a larger extent (and hence be “softer” in momentum space). For these reasons we consider only that part of the density due to the distribution of valence quarks. This argument is by no means new (see e.g. Maekawa and Robilotta [40] for the case of one-pion exchange as well as Refs. [41, 42, 43]). Form factors of the mesonic dressing type have been extensively studied (see e.g. Ref. [44]).

The non-relativistic form factor can be obtained directly by calculating the Fourier transform of the density (see e. g. Ref. [17]). While more realistic forms are possible, we assume here an exponential density in the center of mass of the nucleon corresponding to a dipole form factor of the type

$$\frac{(\Lambda^2 - \mu^2)^2}{(\mathbf{q}^2 + \Lambda^2)^2} = \left( \frac{\Lambda^2 - \mu^2}{\Lambda^2} \right)^2 \left( \frac{\Lambda^2}{\mathbf{q}^2 + \Lambda^2} \right)^2 \quad (71)$$

if we chose to normalize the form factor to unity at the nucleon pole and we have neglected the small recoil correction,  $\mu^4/(4m^2)$ , to  $-\mu^2$ . The spatial distribution corresponding to this form is proportional to  $e^{-\Lambda r}$ . It is well known that

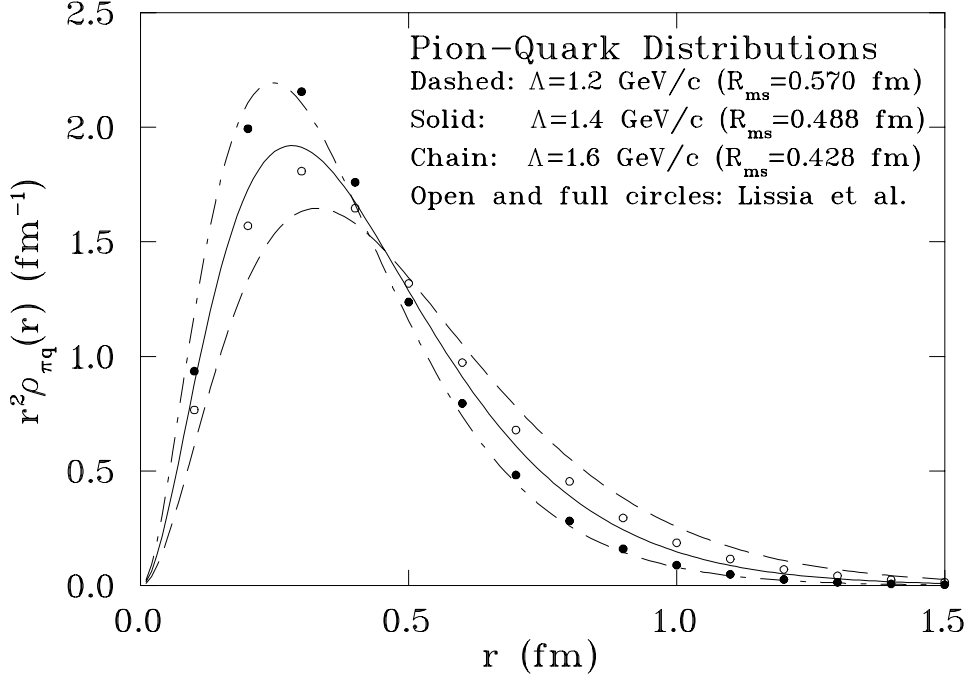


FIG. 4: Comparison with distributions arising from the dipole form factor with those obtained from the lattice calculations of Lissia et al. [45] by the procedures given in the text.

there is a problem with this density since it has a finite derivative with respect to  $r$  at the origin but this presumably only causes significant corrections at very high momenta. The value of  $\Lambda = 1.4$  GeV most often used in our calculations corresponds to an rms core radius of the exponential density of 0.49 fm.

An exponential shape is indeed suggested by lattice calculations. Lissia et al. [45] gave spatial distributions for the distance between quarks,  $\rho_{qq}(r_{qq})$ , in the nucleon, and the pion and  $\rho$  mesons. To find the distribution about a fixed center,  $\rho_q(r)$  needed here, a conversion must be made. If we assume no correlations between quarks and make no center-of-mass correction (in the same manner as Lissia et al. did to compare with the MIT bag model) the conversion between these two densities is given by the rule that the Fourier transform of  $\rho_{qq}$  is the square of that for  $\rho_q$ . The distributions given in Ref. [45] for  $\rho_{qq}$  are well fit by an exponential,  $e^{-\alpha r_{qq}}$ , except for the smallest values of  $r_{qq}$ , leading to a dipole form factor. The square root of this form factor gives a monopole form factor with the same value of  $\alpha$ . Since the pion-nucleon interaction will be governed by a convolution of the pion and nucleon distributions, or a product of the form factors, the result of this type of conversion is the product of two monopole form factors, or, if the ranges are the same, a single dipole form factor. The ranges we extract from the figures in Ref. [45] are  $\alpha = 7.0 \text{ fm}^{-1}$  for the proton and  $\beta = 6.4 \text{ fm}^{-1}$  for the pion. If we were to take both ranges to be  $7.0 \text{ fm}^{-1}$  the result would be a dipole form factor with a range very nearly 1.4 GeV/c which is what we have used in most of the calculations shown. For two different values of the ranges the density is given by

$$\rho_{\pi q}(r) = \frac{\alpha^2 \beta^2}{\beta^2 - \alpha^2} \frac{(e^{-\alpha r} - e^{-\beta r})}{r}. \quad (72)$$

This density is shown by the open circles in Fig. 4 compared with densities resulting from dipole form factors, i.e. pure exponentials. The the root mean square radius,  $R_{ms}$ , corresponding to this distribution is 0.52 fm.

Another possibility for the conversion of the pion distribution is to take the distance to the center of mass to be half the distance between quarks. This choice leads to a product form factor

$$\frac{\alpha^2}{\alpha^2 + \mathbf{q}^2} \left( \frac{\beta^2}{\beta^2 + \mathbf{q}^2} \right)^2, \quad (73)$$

where the  $\beta$  is twice the value found in the fit to  $\rho_{qq}$ . This form factor gives the density

$$\rho_{\pi q}(r) = \frac{\alpha^2 \beta^4}{r(\beta^2 - \alpha^2)^2} \left[ e^{-\alpha r} - e^{-\beta r} - \frac{(\beta^2 - \alpha^2)r}{2\beta} e^{-\beta r} \right], \quad (74)$$

which is shown as the solid dots in Fig. 4. The  $R_{ms}$  corresponding to this density is 0.44 fm.

Alexandrou et al. [46] also made calculations of  $\rho_{qq}$  and commented that their distributions were very well fit with an exponential form. In a variety of calculations they found  $R_{rms}$  values of the pion-proton system in the range from 0.55 to 0.60 fm.

Another estimate of this radius can be obtained directly from form factors for pion-nucleon coupling. For a monopole form factor, a value of  $\Lambda$  of 800 MeV to 1 GeV was found [47]. Choosing an equivalent rms radius leads to values in the range 1.13 to 1.41 GeV/c for a dipole form.

While the original MIT bag model used a radius near 1 fm. (for all of the constituents of the nucleon), corrections due to the inclusion of a pion cloud and the recoil degree of freedom made by Bolsterli and Parmentola [48] led to values of the rms radius near 0.45 fm.

### B. Relativistic Generalization

One often attempts to make a generalization of Eq. (71) to a relativistic dependence on momentum of the type

$$\frac{(\Lambda^2 - \mu^2)^2}{(q_0^2 - \mathbf{q}^2 - \Lambda^2)^2}, \quad (75)$$

i.e.  $-\mathbf{q}^2 \rightarrow q^2 = q_0^2 - \mathbf{q}^2$ . While this substitution makes the form factor invariant, it is not the only way to achieve this objective. This procedure introduces additional singularities on the real axis in  $q_0$  which are often regarded as spurious.

We suppose that the distribution of quarks is known in the rest frame of the nucleon and assume it to be spherically symmetric with its Fourier transform being a function of the square of the conjugate momentum,  $\mathbf{t}^2$ . This distribution should be boosted into the center of mass system of the two nucleons but a boost is only defined for on-shell particles.

On general principle, to preserve Lorentz invariance, the form factor should be a function of Lorentz scalars only. In the case of a pion-nucleon vertex (neglecting spin) there are three four-vectors to work with, the initial and final nucleon momenta and the pion momentum. Due to 4-momentum conservation only two are independent. Let us choose the initial nucleon momenta ( $\mathbf{k}$ ) and the pion momentum ( $\mathbf{q}$ ). From them we can construct three scalars  $q^2$ ,  $k^2$ , and  $k \cdot q$ .

We expect the desired invariant to involve the nucleon momentum if it is to represent a boost into the nucleon rest frame in the on-shell limit. Working with these invariants and taking into account that there should be scaling with the dimensions of  $\mathbf{q}$ , to evaluate to  $\mathbf{t}^2$ , the expression should be bilinear in  $\mathbf{q}$ . Since  $k \cdot q$  is linear in  $\mathbf{q}$  we must use its square, which implies that, in order to be coherent in  $\mathbf{k}$  as well, the only two invariants to consider are  $(k \cdot q)^2$  and  $k^2 q^2$ . The linear combination

$$(k \cdot q)^2 - k^2 q^2 \equiv m^2 Z^2(k, q) \quad (76)$$

indeed reduces to  $m^2 \mathbf{t}^2 = m^2 \mathbf{q}^2$  when the nucleon four-momentum,  $\mathbf{k}$ , is taken to be  $(m, 0)$ . We shall adopt the variable  $Z^2(k, q)$ , which provides an off-shell generalization of the boost to the nucleon rest frame, to replace  $\mathbf{q}^2$  in Eq. (71). For a discussion of the Lorentz tensor which represents the 4-dimensional cross product of  $\mathbf{k}$  and  $\mathbf{q}$  and can be contracted to form  $Z^2$  see appendix C.

### C. Singularities in $q_0$

The problem of the possible unwanted poles in  $q_0$  on the real axis is at least partially resolved since the condition for a singularity  $(k \cdot q)^2 - k^2 q^2 + m^2 \Lambda^2 = 0$  gives as roots for  $q_0$

$$q_0 = \frac{k_0 \mathbf{k} \cdot \mathbf{q} \pm \sqrt{-\{k^2 [\mathbf{k}^2 \mathbf{q}^2 - (\mathbf{k} \cdot \mathbf{q})^2] + \mathbf{k}^2 m^2 \Lambda^2\}}}{\mathbf{k}^2}. \quad (77)$$

As long as the nucleon remains time-like ( $k^2 > 0$ ) the quantity under the radical is negative so that there is no zero on the real axis. Since, for the exchange of two pions, at least one of the nucleons at each vertex is on shell, and there is no zero on the real axis for  $q_0$  for the nucleon momentum on shell, the problem of unwanted additional singularities is resolved.

Poles do exist in the complex plane and lead a finite value of the principal-value integral on  $q_0$  (an integral over only poles on the real axis will lead to a principal value contribution of zero). Since, if the pole is very far from the real axis its contribution will become negligible, in the limit of  $\Lambda \rightarrow \infty$  the principal-value part of the  $q_0$  integral vanishes as expected. We can see from Eq. (77) that in the limit of  $\mathbf{k} \rightarrow 0$  the pole also moves far from the real axis so at low energies the principal-value contribution tends to zero.

Such poles in the upper half of the complex plane are often considered to lead to a violation of causality. In the present case we are considering a pair of finite-size particles which are described in terms of the motion of their centers. Hence, they can start to interact when they are a distance apart equal to twice their radii. The usual considerations of causality [37, 38, 39] deal with two point particles and the expectation that any interaction between them can not propagate faster than the speed of light. This criterion does not apply to the present case since the points which need to be connected by the speed of light are not the centers but any co-moving points included in their structure. The scattered wave can start to appear before the centers of the distributions can be connected by a light ray. The appearance of these poles is natural and expected. Of course, their contribution tends to zero as the size of the system goes to zero ( $\Lambda \rightarrow \infty$ ).

Since the size of the system becomes unmeasurable at very low energy we should expect that the nucleons could be treated as point particles in this regime so that we expect that standard causality will be valid in the low-energy limit. We see that, since the pole off of the real axis gives a negligible contribution in this region being very far from the real axis this expectation is realized.

#### D. Properties of $Z^2$

The function  $Z^2$  has the property

$$Z^2(p \pm q, q) = Z^2(p, q) \text{ or, in particular } Z^2(k', q) = Z^2(k, q). \quad (78)$$

Since  $Z^2$  is independent of the use of the initial or final nucleon momentum, the vertex function is a property of the vertex itself and not of the individual four-momenta. If the three 4-momenta which are connected to the vertex are  $p_1$ ,  $p_2$  and  $p_3$  with a conservation law between them, say  $p_3 = \pm p_1 \pm p_2$ , then any two of the momenta can be used for the evaluation of the vertex function, i.e.

$$Z^2(p_1, p_2) = Z^2(p_1, p_3) = Z^2(p_3, p_2) = \dots \quad (79)$$

An equivalent way to express this function is

$$Z^2 = \frac{[p_1^2]^2 + [p_2^2]^2 + [p_3^2]^2 - 2(p_1^2 p_2^2 + p_1^2 p_3^2 + p_2^2 p_3^2)}{4m^2}. \quad (80)$$

In a more general view, there are two invariants available;  $(k \cdot q)^2/m^2$ , which evaluates to  $q_0^2$  in the rest frame of the nucleon and  $\frac{(k \cdot q)^2 - k^2 q^2}{m^2}$  which evaluates to  $\mathbf{q}^2$  in this rest frame. One could choose any combination of  $\mathbf{q}^2$  and  $q_0^2$  desired for the dependence in the rest frame. However, only  $[(k \cdot q)^2 - k^2 q^2]/m^2$  (and  $q^2$  by dint of containing no reference to the nucleon momentum at all) are independent of which nucleon momentum ( $k$  or  $k'$ ) is used.

The use of the form factor obtained from the Fourier transform of the density in the nucleon center of mass without any dependence on  $q_0$  corresponds to an interaction which is instantaneous in time. This is perhaps to be expected since the valence quarks are always present for interaction, whereas the interaction through the intermediate step of the emission of a meson requires a time  $\hbar/\text{Mass}$  for the meson to be formed and propagate.

Other authors [49, 50] have used relativistic generalizations of the form factor. In particular Ramalho, Arriaga and Peña [49] have argued that the first type of form factor dependence, Eq. (75) corresponds to the dressing of the nucleon by mesons of mass  $\Lambda$  and suggest that the variable  $\mathbf{q}^2$  should be replaced by

$$Q^2 \equiv \frac{(P \cdot q)^2}{P^2} - q^2, \quad (81)$$



where  $P$  is the center-of-mass momentum of the two nucleons. The value of  $Q^2$  evaluates to  $\mathbf{q}^2$  in the center of mass system so that there is no dependence on  $q_0$  if one calculates in that reference frame, hence no possible singularity in that variable. This may be a useful form but the underlying basis in physics is not clear since the form factor should be a property of the pion-nucleon vertex and not the entire system. How a pion interacts with a single nucleon should not depend on the momentum of a second nucleon.

### E. Conditions on the Form Factor

Reviewing the previous paragraphs, we may summarize the desired properties of an off-shell form factor arising from an extended source.

1. There should be no poles of  $q_0$  on the real axis.
2. For the case of the nucleon on shell and at rest, the form factor should be independent of  $q_0$  so that the interaction is instantaneous.
3. As the nucleon energy approaches zero, poles in  $q_0$  should tend to  $\pm i\infty$ . This is necessary since, in this limit, the interaction could be regarded as being among point particles and, by causality, there can be no contribution from poles off of the real axis. While the arguments of the previous point and this one arise from different physical bases, they are mathematically related.

For a typical example consider a form factor of the type

$$\frac{\Lambda^2}{aq_0^2 + bq_0 + \mathbf{q}^2 + \Lambda^2}, \quad (82)$$

where  $a$  and  $b$  are real functions of  $\mathbf{q}$ ,  $\mathbf{k}$  and  $k_0$ . The poles in  $q_0$  will be given by

$$q_0 = \frac{-b \pm \sqrt{b^2 - 4a(\mathbf{q}^2 + \Lambda^2)}}{2a}. \quad (83)$$

In order that  $q_0 \rightarrow \pm i\infty$  as  $|\mathbf{k}| \rightarrow 0$  both  $a$  and  $b$  must tend to zero in this limit. This, in turn, means that the form factor becomes independent of  $q_0$  in the limit  $|\mathbf{k}| \rightarrow 0$ .

4. In the nucleon rest frame the form factor (which is a function of  $|\mathbf{q}|^2$  only) is the Fourier transform of the source density, a positive definite function.

### F. Application to the present case.

For the application of the form factor in the present calculation we can always choose the nucleon to be one of the external lines and hence on shell with energy  $E$ . If we define

$$f(E, \mathbf{k}, q_0, \mathbf{q}) = f(k, q) = \left[ \frac{\Lambda^2 - \mu^2}{\frac{(k \cdot q)^2}{m^2} - q^2 + \Lambda^2} \right]^2, \quad (84)$$

a product of four of these factors will appear, one for each vertex. For the box diagram we have

$$\mathcal{F} = f(E, \mathbf{k}, q_0, \mathbf{q}) f(E, -\mathbf{k}, q_0, \mathbf{q}) f(E, \mathbf{k}', q_0, \mathbf{q}') f(E, -\mathbf{k}', q_0, \mathbf{q}'), \quad (85)$$

while for the crossed diagram the product

$$\mathcal{F} = f(E, \mathbf{k}, q_0, \mathbf{q}') f(E, -\mathbf{k}, q_0, \mathbf{q}) f(E, \mathbf{k}', q_0, \mathbf{q}) f(E, -\mathbf{k}', q_0, \mathbf{q}') \quad (86)$$

enters. Since these functions are scalars and do not have any poles on the real axis, the manipulation of the spin observables and the treatment of the singularities is not affected by their presence.

## V. DISPERSION RELATION APPROACH

In order to cross-check our Feynman diagram results we have calculated the two-pion exchange in the dispersion relation approach following Ref. [25]. The matrix element  $\mathcal{M}$  of Eq. (1) in section II can be written as,

$$\mathcal{M} = \sum_{i=1}^5 [3p_i^+(w, t, \bar{t}) + 2p_i^-(w, t, \bar{t}) \boldsymbol{\tau}_1 \cdot \boldsymbol{\tau}_2] P_i. \quad (87)$$

Here,  $w, t, \bar{t}$  are the Mandelstam invariants satisfying  $w + t + \bar{t} = 4m^2$ ,  $\boldsymbol{\tau}_{1(2)}$  the isospin Pauli matrices for the nucleon 1(2) and  $P_i$  the perturbative invariants. One has,

$$w = (k_1 + k_2)^2, \quad t = (k_1 - k'_1)^2, \quad \bar{t} = (k_1 - k'_2)^2 \quad (88)$$

and

$$\begin{aligned} P_1 &= 1^1 1^2, \\ P_2 &= -[(\gamma^1 \cdot N) 1^2 + (\gamma^2 \cdot P) 1^1], \\ P_3 &= (\gamma^1 \cdot N) (\gamma^2 \cdot P), \\ P_4 &= \gamma^1 \cdot \gamma^2, \\ P_5 &= \gamma_5^1 \gamma_5^2, \end{aligned} \quad (89)$$

with

$$N = \frac{1}{2} (k_2 + k'_2), \quad P = \frac{1}{2} (k_1 + k'_1). \quad (90)$$

Assuming the Mandelstam representation [51], the two-pion exchange invariant amplitudes  $p_i^\pm(w, t, \bar{t})$  of Eq. (87) satisfy the following double dispersion relations,

$$\begin{aligned} p_i^\pm(w, t, \bar{t}) &= \frac{1}{\pi^2} \int_{4\mu^2}^{+\infty} \frac{dt'}{t' - t - i\epsilon} \int_{4m^2}^{+\infty} \frac{dw'}{w' - w - i\epsilon} y_i^\pm(w', t') \\ &\mp (-1)^i \frac{1}{\pi^2} \int_{4\mu^2}^{+\infty} \frac{dt'}{t' - t - i\epsilon} \int_{4m^2}^{+\infty} \frac{dw'}{w' - \bar{t} - i\epsilon} y_i^\pm(w', t'), \end{aligned} \quad (91)$$

where the  $y_i^\pm(w, t)$  are the double spectral functions. In Eq. (91) the first double integrals represent the contributions of the two-pion-exchange box diagram (see Fig. 2). The second double integrals give the contribution of the crossed-pion diagram (Fig. 3). They are obtained from the contributions of the box diagram by the substitution  $k_1 \leftrightarrow -k'_1$  which is equivalent to that of  $w \leftrightarrow \bar{t}$ . This substitution changes the sign of the invariants  $P_1, P_3, P_5$  while  $P_2$  and  $P_4$  are not modified. It also changes the isospin dependence. These changes result in the signs given here. We shall show below how one can calculate the two-pion-exchange double spectral functions  $y_i^\pm(w, t)$ . Use of the following decomposition

$$\begin{aligned} \frac{1}{t - t' - i\epsilon} \frac{1}{w' - (4m^2 - w - t) - i\epsilon} &= \frac{1}{t - t' - i\epsilon} \frac{1}{w' - (4m^2 - w - t') - i\epsilon} \\ &+ \frac{1}{w' - (4m^2 - w - t) - i\epsilon} \frac{1}{t' - (4m^2 - w - w') - i\epsilon} \end{aligned} \quad (92)$$

allows us to write Eq. (91) as

$$\begin{aligned}
p_i^\pm(w, t, \bar{t}) &= \frac{1}{\pi} \int_{4\mu^2}^{+\infty} \frac{dt'}{t' - t - i\epsilon} [\rho_i^\pm(w, t') \mp (-1)^i \rho_i^\pm(4m^2 - w - t', t')] \\
&\mp (-1)^i \frac{1}{\pi} \int_{4m^2}^{+\infty} \frac{dw'}{w' - \bar{t} - i\epsilon} a_i^\pm(w', 4m^2 - w - w'),
\end{aligned} \tag{93}$$

with

$$\rho_i^\pm(w, t) = \text{Im}_t p_i^\pm(w, t) = \frac{1}{\pi} \int_{4m^2}^{+\infty} \frac{dw'}{w' - w - i\epsilon} y_i^\pm(w', t), \tag{94}$$

and

$$a_i^\pm(w', 4m^2 - w - w') = \frac{1}{\pi} \int_{4\mu^2}^{+\infty} \frac{dt'}{t' - (4m^2 - w - w') - i\epsilon} y_i^\pm(w', t'). \tag{95}$$

Since the term with  $a_i^\pm(w', 4m^2 - w - w')$  in Eq. (93) gives rise to a rather short range force with mass exchanges larger than  $2m$  it was neglected in the Paris Potential [25, 26, 27]. In Eq. (94) the notation  $\text{Im}_t$  comes from the use of the relation

$$\frac{1}{t' - t - i\epsilon} = \frac{P}{t' - t} + i\pi\delta(t' - t), \tag{96}$$

where  $P$  indicates the principal value part of the integral.

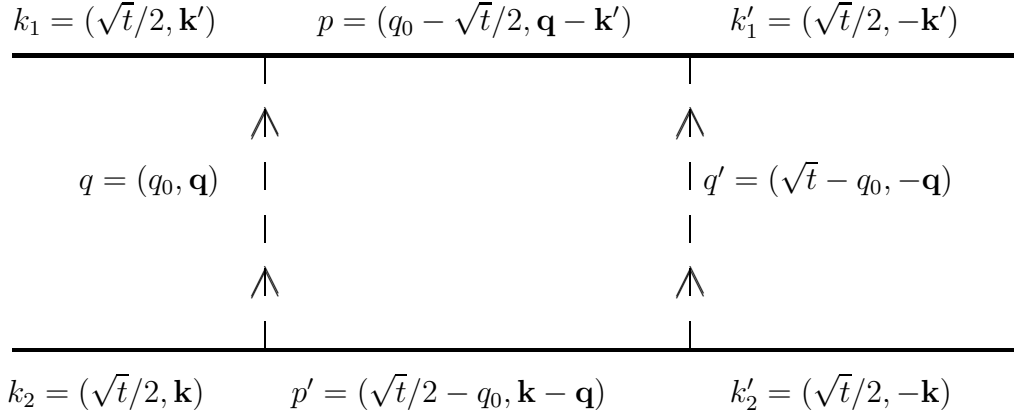


FIG. 5: Box diagram kinematics in the t-channel c.m..

The unitarity condition in the t-channel for the  $N\bar{N} \rightarrow 2\pi \rightarrow N\bar{N}$  process [27] leads to

$$\begin{aligned}
\sum_i [\rho_i^\pm(w, t) \mp (-1)^i \rho_i^\pm(4m^2 - w - t, t)] P_i = \\
\frac{1}{128\pi^2} \sqrt{\frac{t - 4\mu^2}{t}} \int d\Omega_Q [A_1^{*\pm}(s_1, t, \bar{s}_1) 1^1 + \boldsymbol{\gamma}^1 \cdot \mathbf{Q} B_1^{*\pm}(s_1, t, \bar{s}_1)] [A_2^\pm(s_2, t, \bar{s}_2) 1^2 + \boldsymbol{\gamma}^2 \cdot \mathbf{Q} B_2^\pm(s_2, t, \bar{s}_2)],
\end{aligned} \tag{97}$$

where the four-momenta of the on-shell exchanged pions, in their t-channel center of mass (see the kinematics given in Fig. 5), are,

$$q = \left( \frac{\sqrt{t}}{2}, -\mathbf{Q} \right), \quad q' = \left( \frac{\sqrt{t}}{2}, \mathbf{Q} \right). \tag{98}$$

The amplitudes  $A(B)_{1(2)}^\pm(s_{1(2)}, t, \bar{s}_{1(2)})$  are the usual invariants for the reaction  $N\bar{N} \rightarrow \pi\pi$  [52]. The Mandelstam invariants  $s_{1(2)}$ ,  $t$  and  $\bar{s}_{1(2)}$ , satisfying,  $s_{1(2)} + t + \bar{s}_{1(2)} = 2m^2 + 2\mu^2$ , are

$$\begin{aligned} s_1 &= (k_1 - q')^2 = m^2 + \mu^2 - \frac{t}{2} - 2\mathbf{P} \cdot \mathbf{Q}, \\ t &= (k_1 - k'_1)^2 = 4(\mathbf{Q}^2 + \mu^2), \\ \bar{s}_1 &= (k_1 + q)^2 = m^2 + \mu^2 - \frac{t}{2} + 2\mathbf{P} \cdot \mathbf{Q} \end{aligned} \quad (99)$$

and

$$s_2 = (k_2 - q)^2 = m^2 + \mu^2 - \frac{t}{2} - 2\mathbf{N} \cdot \mathbf{Q}, \quad \bar{s}_2 = (k_2 + q')^2 = m^2 + \mu^2 - \frac{t}{2} + 2\mathbf{N} \cdot \mathbf{Q}, \quad (100)$$

with,  $q^2 = q'^2 = \mu^2 = \frac{t}{4} - \mathbf{Q}^2$ . Expressions (99) and (100) follow from

$$\begin{aligned} k_1 &= \left(-\frac{\sqrt{t}}{2}, \mathbf{k}_1\right), & k'_1 &= \left(\frac{\sqrt{t}}{2}, \mathbf{k}_1\right), \\ k_2 &= \left(\frac{\sqrt{t}}{2}, \mathbf{k}_2\right), & k'_1 &= \left(-\frac{\sqrt{t}}{2}, \mathbf{k}_2\right), \\ P &= (0, \mathbf{k}_1), & N &= (0, \mathbf{k}_2), \end{aligned} \quad (101)$$

since  $\mathbf{k}_2 - \mathbf{k}'_2 = \mathbf{q} - \mathbf{q}' = \mathbf{k}'_1 - \mathbf{k}_1 = 0$  (see Fig. 5 and Eq.(90)). Introducing the four-vector  $L_\lambda = \varepsilon_{\lambda\nu\rho\sigma} M^\nu K^\rho \Delta^\sigma$ , where,

$$\begin{aligned} M &= N + P = (0, \mathbf{N} + \mathbf{P}), \\ K &= N - P = (0, \mathbf{N} - \mathbf{P}), \\ \Delta &= k'_1 - k_1 = (\sqrt{t}, 0), \end{aligned} \quad (102)$$

$Q$  can be represented as

$$Q = \frac{Q \cdot M}{M^2} M + \frac{Q \cdot K}{K^2} K + \frac{Q \cdot \Delta}{\Delta^2} \Delta + \frac{Q \cdot L}{L^2} L. \quad (103)$$

Eq. (97) can then be decomposed in the invariants  $P_i$  of Eq. (89) as [27, 53],

$$\begin{aligned} \sum_i [\rho_i^\pm(w, t) \mp (-1)^i \rho_i^\pm(4m^2 - w - t, t)] P_i &= \frac{1}{128\pi^2} \sqrt{\frac{t - 4\mu^2}{t}} \\ &\times [(\mathcal{A}^\pm + 2m\mathcal{C}^\pm + m^2\mathcal{E}^\pm) P_1 + (\mathcal{B}^\pm + m\mathcal{D}^\pm) P_2 + \mathcal{E}^\pm P_3 - \mathcal{F}^\pm P_4], \end{aligned} \quad (104)$$

with

$$\begin{aligned}
\mathcal{A}^\pm &= \int d\Omega_Q A_1^{*\pm} A_2^\pm, \\
\mathcal{B}^\pm &= \int d\Omega_Q B_1^{*\pm} A_2^\pm \left( \frac{Q \cdot M}{M^2} + \frac{Q \cdot K}{K^2} \right), \\
\mathcal{C}^\pm &= \int d\Omega_Q B_1^{*\pm} A_2^\pm \left( \frac{Q \cdot M}{M^2} - \frac{Q \cdot K}{K^2} \right), \\
\mathcal{D}^\pm &= \frac{1}{M^2 K^2} \int d\Omega_Q B_1^{*\pm} B_2^\pm \left[ \frac{(Q \cdot M)^2}{M^2} (2K^2 + M^2) + \frac{(Q \cdot K)^2}{K^2} (K^2 + 2M^2) - Q^2 (K^2 + M^2) \right], \\
\mathcal{E}^\pm &= \frac{1}{M^2 K^2} \int d\Omega_Q B_1^{*\pm} B_2^\pm \left[ \frac{(Q \cdot M)^2}{M^2} (2K^2 - M^2) + \frac{(Q \cdot K)^2}{K^2} (K^2 - 2M^2) - Q^2 (K^2 - M^2) \right], \\
\mathcal{F}^\pm &= \int d\Omega_Q B_1^{*\pm} B_2^\pm \left[ -Q^2 + \frac{(Q \cdot M)^2}{M^2} + \frac{(Q \cdot K)^2}{K^2} \right].
\end{aligned} \tag{105}$$

Here  $M^2 = w$  and  $K^2 = \bar{t} = 4m^2 - w - t$ . Note that the Bjorken-Drell metric used here leads to some sign differences with respect to references [27, 53] where the Pauli metric was used.

#### A. Nucleon Pole Contribution for Pseudo-scalar Coupling

If the invariant amplitudes  $A(B)_{1(2)}^\pm$  are expressed as fixed- $t$  dispersion relations [52] one can write the  $\rho_i^\pm$  given by Eqs. (104) and (105) in the spectral form (94). Following Ref. [54] one can use the Cutkosky rules [55] to calculate the imaginary part of the  $\rho_i^\pm$  from Eq. (105). The expressions for the  $y_i^\pm(w, t)$  of Eq. (94) in terms of double integrals over  $s_1$  and  $s_2$  on quantities depending on elastic pion-nucleon scattering absorptive parts, are given by Eqs. (2.6) to (2.8) of Ref. [25]. The double spectral functions  $y_{i,N}^\pm(w, t)$  of the box diagram for pseudo-scalar (PS) pion-nucleon coupling can then be obtained from these equations. In this case the  $A(B)_{1(2),PS}^\pm$  for the  $\pi N$  nucleon Born term are (see e.g. Eq. (A.6.30) of Ref. [52]),

$$A_{1(2),PS}^\pm = 0, \quad B_{1(2),PS}^\pm = g^2 \left( \frac{1}{m^2 - s_{1(2)} - i\epsilon} \mp \frac{1}{m^2 - \bar{s}_{1(2)} - i\epsilon} \right). \tag{106}$$

The absorptive parts of  $A_{1(2),PS}^\pm$  are zero and those of  $B_{1(2),PS}^\pm$  are given by  $\pi g^2 \delta(s_{1(2)} - m^2)$  for the direct term leading to,

$$\begin{aligned}
y_{1,N}^\pm(w, t) &= \pm \frac{\pi^2}{2} \left( \frac{g^2}{4\pi} \right)^2 \frac{m^2}{\sqrt{t}} \frac{K(w, t)}{(4m^2 - t - w)^2} \left[ \frac{4m^2 - 2w - t}{w^2 K(w, t)^2} + (t - 2\mu^2)^2 \right], \\
y_{2,N}^\pm(w, t) &= \pm \frac{\pi^2}{2} \left( \frac{g^2}{4\pi} \right)^2 \frac{m}{\sqrt{t}} \frac{K(w, t)}{(4m^2 - t - w)^2} \left[ -\frac{4m^2 - t}{w^2 K(w, t)^2} + (t - 2\mu^2)^2 \right], \\
y_{3,N}^\pm(w, t) &= \frac{y_1^\pm(w, t)}{m^2}, \\
y_{4,N}^\pm(w, t) &= \pm \frac{\pi^2}{2} \left( \frac{g^2}{4\pi} \right)^2 \frac{1}{\sqrt{t}} K(w, t) \left[ -\frac{1}{w(4m^2 - t - w) K(w, t)^2} \right], \\
y_{5,N}^\pm(w, t) &= 0,
\end{aligned} \tag{107}$$

with

$$K(w, t) = w^{-1/2} [(t - 4\mu^2)(w - 4m^2) - 4\mu^4]^{-1/2}. \quad (108)$$

We define,

$$A(y, t') = \int_{x_0}^{+\infty} \frac{dw'}{w' - y} K(w', t'), \quad C(y, t') = \int_{x_0}^{+\infty} \frac{dw'}{(w' - y)^2} K(w', t') \quad (109)$$

where  $x_0$  is the lower limit of the  $w'$  integration such that  $K(w', t')$  is defined, i. e.,  $(t' - 4\mu^2)(w' - 4m^2) - 4\mu^4 \geq 0$ , which leads to,

$$x_0(t') = 4m^2 + \frac{4\mu^4}{t' - 4\mu^2} \geq 4m^2. \quad (110)$$

With the definition,

$$\eta(w', t') = 4\mu^4 - (t' - 4\mu^2)(w' - 4m^2) = (x_0 - w')(t' - 4\mu^2), \quad (111)$$

we have [56],

$$\rho_1^\pm(w, t') = \rho_{11}^\pm(w, t') - \rho_{12}^\pm(w, t') \quad (112)$$

with

$$\begin{aligned} \rho_{11}^\pm(w, t') &= \pm \frac{\pi}{2} \left( \frac{g^2}{4\pi} \right)^2 \frac{m^2}{\sqrt{t'}} \frac{(t' - 2\mu^2)^2}{4m^2 - w - t'} \left[ \frac{A(w, t') - A(4m^2 - t', t')}{4m^2 - w - t'} + C(4m^2 - t', t') \right], \\ \rho_{12}^\pm(w, t') &= \pm \frac{\pi}{2} \left( \frac{g^2}{4\pi} \right)^2 \frac{m^2}{\sqrt{t'}} [\mathcal{F}_1 A(0, t') + \mathcal{F}_2 A(w, t') + \mathcal{F}_3 C(4m^2 - t', t') + \mathcal{F}_4 A(4m^2 - t', t')]. \end{aligned} \quad (113)$$

The  $\mathcal{F}_i$  are given by,

$$\begin{aligned} \mathcal{F}_1 &= -\frac{4[m^2(t' - 4\mu^2) + \mu^4]}{w(4m^2 - t')}, & \mathcal{F}_2 &= -\frac{\eta(w, t')(2w + t' - 4m^2)}{w(w + t' - 4m^2)^2}, \\ \mathcal{F}_3 &= -\frac{(t' - 2\mu^2)^2}{4m^2 - w - t'}, & \mathcal{F}_4 &= -\mathcal{F}_1 - \mathcal{F}_2. \end{aligned} \quad (114)$$

The expression for  $\rho_2^\pm(w, t')$  is,

$$\rho_2^\pm(w, t') = \rho_{21}^\pm(w, t') + \rho_{22}^\pm(w, t') \quad (115)$$

with

$$\begin{aligned} \rho_{21}^\pm(w, t') &= \frac{\rho_{11}^\pm(w, t')}{m}, \\ \rho_{22}^\pm(w, t') &= \pm \frac{\pi}{2} \left( \frac{g^2}{4\pi} \right)^2 \frac{m}{\sqrt{t'}} (t' - 4m^2) [\mathcal{G}_1 A(0, t') + \mathcal{G}_2 A(w, t') + \mathcal{G}_3 C(4m^2 - t', t') + \mathcal{G}_4 A(4m^2 - t', t')] \end{aligned} \quad (116)$$

and,

$$\begin{aligned} \mathcal{G}_1 &= -\frac{\mathcal{F}_1}{4m^2 - t'}, & \mathcal{G}_2 &= \frac{\mathcal{F}_2}{2w + t' - 4m^2}, \\ \mathcal{G}_3 &= \frac{\mathcal{F}_3}{4m^2 - t'}, & \mathcal{G}_4 &= -\mathcal{G}_1 - \mathcal{G}_2. \end{aligned} \quad (117)$$

Furthermore,

$$\rho_3^\pm(w, t') = \frac{\rho_1^\pm(w, t')}{m^2}, \quad (118)$$

$$\rho_4^\pm(w, t') = \pm \frac{\pi^2}{2} \left( \frac{g^2}{4\pi} \right)^2 \frac{1}{\sqrt{t'}} \frac{1}{4m^2 - w - t'} [\eta(w, t') A(w, t') - (t' - 2\mu^2)^2 A(4m^2 - t', t')]. \quad (119)$$

The functions  $A(y, t')$  and  $C(y, t')$  can be calculated analytically. First notice that,

$$C(y, t') = -\frac{\sqrt{t' - 4\mu^2}}{(t' - 4m^2)(t' - 2\mu^2)^2} + \frac{(t' - 4\mu^2)(2t' - 4m^2) + 4\mu^4}{(t' - 4m^2)(t' - 2\mu^2)^2} A(y, t'), \quad (120)$$

$$A(y, t') = \int_{x_0}^{+\infty} \frac{K(w', t')}{w' - y - i\epsilon} dw' = P \int_{x_0}^{+\infty} \frac{K(w', t')}{w' - y} dw' + i\pi K(y, t'). \quad (121)$$

One obtains Eq. (121) using Eq. (96). Depending on the value of  $y$  one has the following results:

- if  $y < 0$ , then  $\eta(y, t') = (x_0 - y)(t' - 4\mu^2) > 0$

$$A(y, t') = \frac{1}{\sqrt{-\eta(y, t')y}} \ln \frac{1 + \sqrt{\frac{-y(t' - 4\mu^2)}{\eta(y, t')}}}{1 - \sqrt{\frac{-y(t' - 4\mu^2)}{\eta(y, t')}}} = \frac{1}{\sqrt{-\eta(y, t')y}} \ln \frac{1 + \sqrt{\frac{y}{y - x_0}}}{1 - \sqrt{\frac{y}{y - x_0}}}, \quad (122)$$

- if  $0 < y < x_0$ , then  $\eta(y, t') > 0$  and

$$A(y, t') = \frac{2}{\sqrt{\eta(y, t')y}} \arctan \sqrt{\frac{y(t' - 4\mu^2)}{\eta(y, t')}} = \frac{2}{\sqrt{\eta(y, t')y}} \arctan \sqrt{\frac{y}{x_0 - y}}, \quad (123)$$

- if  $y > x_0$ , then  $\eta(y, t') < 0$ ,  $A$  has an imaginary part:

$$\text{Re}A(y, t') = -\frac{1}{\sqrt{-\eta(y, t')y}} \ln \frac{1 + \sqrt{\frac{-y(t' - 4\mu^2)}{\eta(y, t')}}}{\sqrt{\frac{-y(t' - 4\mu^2)}{\eta(y, t')}} - 1} = -\frac{1}{\sqrt{-\eta(y, t')y}} \ln \frac{1 + \sqrt{\frac{y}{y - x_0}}}{\sqrt{\frac{y}{y - x_0}} - 1}, \quad (124)$$

$$\text{Im}A(y, t') = K(y, t').$$

It can be seen from Eqs. (122) and (123) that  $A$  is continuous at  $y=0$  with the value,

$$A(0, t') = \frac{2\sqrt{t' - 4\mu^2}}{\eta(0, t')w}. \quad (125)$$

On the other hand,  $A$  is discontinuous at  $x_0$ , since taking the limits in Eqs. (123) and (124),

$$\begin{aligned} A(y, t') &\underset{y \rightarrow x_0^-}{\sim} \frac{\pi}{\sqrt{(x_0 - y)(t' - 4\mu^2)y}} \longrightarrow \infty, \\ \lim_{y \rightarrow x_0^+} A(y, t') &= -\frac{1}{y\sqrt{t' - 4\mu^2}}. \end{aligned} \quad (126)$$

This square root divergence will disappear after performing the integration over  $t'$ .

The integration over  $t'$  in Eq. (95) is performed analytically. Let us define,

$$\tilde{K}(w', t') = t'^{-1/2} [(t' - 4\mu^2)(w' - 4m^2) - 4\mu^4]^{-1/2}, \quad (127)$$

$$\tilde{A}(w', \tilde{y}) = \int_{\tilde{x}_0}^{+\infty} \frac{dt'}{t' - \tilde{y}} \tilde{K}(w', t'), \quad \tilde{C}(w', \tilde{y}) = \int_{\tilde{x}_0}^{+\infty} \frac{dt'}{(t' - \tilde{y})^2} \tilde{K}(w', t'), \quad (128)$$

where  $\tilde{x}_0$  is the lower limit of the  $t'$  integration such that  $\tilde{K}(w', t')$  is defined, i. e.,  $(t' - 4\mu^2)(w' - 4m^2) - 4\mu^4 \geq 0$ , which leads to,

$$\tilde{x}_0(t') = 4\mu^2 + \frac{4\mu^4}{w' - 4m^2} \geq 4\mu^2. \quad (129)$$

One obtains, with  $\tilde{y} = 4m^2 - w - w'$  and  $\tilde{w}' = 4m^2 - w'$ ,

$$\begin{aligned} a_1^\pm(w', \tilde{y}) &= \pm \frac{\pi}{2} \left( \frac{g^2}{4\pi} \right)^2 [a_{11}(w', \tilde{y}) + a_{12}(w', \tilde{y})], \\ a_2^\pm(w', \tilde{y}) &= \pm \frac{\pi}{2} \left( \frac{g^2}{4\pi} \right)^2 \left[ \frac{a_{11}(w', \tilde{y})}{m} + \tilde{a}_{12}(w', \tilde{y}) \right], \\ a_3^\pm(w', \tilde{y}) &= \frac{a_1^\pm(w', \tilde{y})}{m^2}, \\ a_4^\pm(w', \tilde{y}) &= \pm \frac{\pi}{2} \left( \frac{g^2}{4\pi} \right)^2 \frac{1}{w\sqrt{w'}} [\eta(w', \tilde{y})\tilde{A}(w', \tilde{y}) - \eta(w', \tilde{w}')\tilde{A}(w', \tilde{w}')]. \end{aligned} \quad (130)$$

In Eq. (130),

$$\begin{aligned} a_{11}(w', \tilde{y}) &= \frac{m^2}{w^2\sqrt{w'}} \left[ (\tilde{y} - 2\mu^2)^2 \tilde{A}(w', \tilde{w}') - (\tilde{w}' - 2\mu^2)(\tilde{y} - w - 2\mu^2) \tilde{A}(w', \tilde{w}') + w(\tilde{w}' - 2\mu^2)^2 \tilde{C}(w', \tilde{w}') \right], \\ a_{12}(w', \tilde{y}) &= \frac{m^2}{w^2w'\sqrt{w'}} \left[ (w - w')\eta(w', \tilde{y})\tilde{A}(w', \tilde{y}) - [w^2 + (w' - w)\eta(w', \tilde{y})]\tilde{A}(w', \tilde{w}') + ww'\eta(w', \tilde{w}')\tilde{C}(w', \tilde{w}') \right], \\ \tilde{a}_{12}(w', \tilde{y}) &= \frac{m}{w^2w'\sqrt{w'}} \left[ (w + w')\eta(w', \tilde{y})\tilde{A}(w', \tilde{y}) + [w^2 - (w + w')\eta(w', \tilde{y})]\tilde{A}(w', \tilde{w}') + ww'\eta(w', \tilde{w}')\tilde{C}(w', \tilde{w}') \right]. \end{aligned} \quad (131)$$

The functions  $\tilde{A}(w', \tilde{y})$  and  $\tilde{C}(w', \tilde{y})$  with  $\tilde{y} \leq 0$  are,

$$\tilde{A}(w', \tilde{y}) = \frac{1}{\sqrt{-\eta(w', \tilde{y})\tilde{y}}} \ln \frac{1 + \sqrt{\frac{\tilde{y}}{\tilde{y} - x_0}}}{1 - \sqrt{\frac{\tilde{y}}{\tilde{y} - x_0}}}, \quad (132)$$

$$\tilde{C}(w', \tilde{y}) = \frac{\sqrt{-\tilde{w}'}}{\tilde{y}\eta(w', \tilde{y})} - \frac{\tilde{w}'(\tilde{y} - 2m^2) + 2\mu^4}{\tilde{y}\eta(w', \tilde{y})} \tilde{A}(w', \tilde{y}). \quad (133)$$

We have calculated the discontinuities of the  $p_i^\pm$  along  $w$ , i. e.,

$$\lim_{\epsilon \rightarrow 0} [p_i(w + i\epsilon, t') - p_i(w - i\epsilon, t')] = 2i \text{Im}_w p_i(w, t') = 2i \frac{1}{\pi} \int_{4\mu^2}^{+\infty} \frac{dt'}{t' - t} \text{Im}_w \rho_i^\pm(w, t'). \quad (134)$$



We introduce the following explicit notations

$$\begin{aligned}\rho_i^{\pm \text{box}}(w, t') &= \text{Re} \rho_i^{\pm}(w, t'), \\ \rho_i^{\pm \text{cro}}(w, t') &= \mp (-1)^i \rho_i^{\pm \text{box}}(w \leftrightarrow 4m^2 - t' - w, t'), \\ \text{Im}_w \rho_i^{\pm \text{box}}(w, t') &= \text{Im}_w \rho_i^{\pm}(w, t') = y_{i,N}^{\pm}(w, t').\end{aligned}\tag{135}$$

Here again, the last equality of Eq. (135) follows from the application of Eq. (96). In the expressions (113), (116), (119) and (124), the imaginary part of the  $\rho_i^{\pm}(w, t')$  comes only from  $A$ . There are only three  $A$  terms:  $A(w, t')$ ,  $A(0, t')$  and  $A(4m^2 - t', t')$  in Eqs. (113) and (116) that have a non-zero imaginary part for  $y > x_0$ . However, from (110) one cannot have  $4m^2 - t' > x_0$ , so, *a fortiori* one cannot have  $4m^2 - t' - w > x_0$  and **only the box diagram has an imaginary part** which justifies the superscript “box” in the expression for the imaginary part. The superscript “cro” denotes the contribution from the crossed diagram. We write

$$p_i^{\pm \text{box}}(w, t) = \frac{1}{\pi} \int_{4\mu^2}^{+\infty} \frac{dt'}{t' - t} \rho_i^{\pm \text{box}}(w, t'),\tag{136}$$

$$\begin{aligned}p_i^{\pm \text{cro}}(\bar{t}, t) &= \frac{1}{\pi} \int_{4\mu^2}^{+\infty} \frac{dt'}{t' - t} \rho_i^{\pm \text{cro}}(\bar{t}, t') \\ &\quad \mp (-1)^i \frac{1}{\pi} \int_{4m^2}^{+\infty} \frac{dw'}{w' - \bar{t}} a_i^{\pm}(w', 4m^2 - w - w'),\end{aligned}\tag{137}$$

$$\text{Im}_w p_i^{\pm}(w, t) = \frac{1}{\pi} \int_{4\mu^2}^{+\infty} \frac{dt'}{t' - t} y_{i,N}^{\pm}(w, t').\tag{138}$$

It can be seen from studying the high  $t'$  behavior of the functions (135) that they decrease like  $1/t'$  or  $\ln(t')/t'$  for  $t' \rightarrow +\infty$ , so that the integrals (136), (137) and (138) on  $t'$  converge. A similar convergence holds for the integrals on  $w'$ . Note that the physical values of  $t(\bar{t})$  being negative, there are no poles in the  $t'(w')$  integration, so there is no further imaginary part. In the present form, the numerical calculation of Eqs. (136), (137) and (138) requires one numerical integration over  $t'$  or  $w'$ .

We have seen (Eq. (126)) that  $A(y, t')$  has a divergence in  $y \rightarrow x_0^-$ . In the expressions for integration on  $t'$ ,  $y$  takes the values  $4m^2 - t'$ , 0,  $4m^2 - t' - w$  and  $w$  (see Eqs. (113), (116) and (135)). The divergence at  $y = x_0$  is in the expression for  $\rho_{11}^{\pm}$  in Eq. (113) where the first argument of  $A$  is  $w$ , so that only the box diagram has this divergence. Fixing  $w$  and using Eq. (110) the condition  $w = x_0$  gives for  $\rho_i^{\pm \text{box}}(w, t')$  a discontinuity at  $t' = t'_0$  with

$$t'_0 = 4\mu^2 + \frac{4\mu^4}{w - 4m^2}.\tag{139}$$

The integral (136) can be split into two pieces,

$$p_i^{\pm \text{box}}(w, t) = \frac{1}{\pi} \int_{4\mu^2}^{t'_0} \frac{dt'}{t' - t} \rho_i^{\pm \text{box}}(w, t') + \frac{1}{\pi} \int_{t'_0}^{+\infty} \frac{dt'}{t' - t} \rho_i^{\pm \text{box}}(w, t').\tag{140}$$

The first integral, of the type,

$$\int_{4\mu^2}^{t'_0} \frac{dt'}{\sqrt{t'_0 - t'}} F(t'),\tag{141}$$

becomes, with  $x = \sqrt{t'_0 - t'}$ ,

$$2 \int_0^{\sqrt{t'_0 - 4\mu^2}} dx F(t'_0 - x^2).\tag{142}$$

This transformation is applied to  $F(t') = \left[ \sqrt{t'_0 - t'} / (\pi(t' - t)) \right] \rho_i^{\pm \text{box}}(w, t')$ . The second integral can be recast into a finite domain by the following change of variable

$$t' = \frac{\lambda(x+1) - 2t'_0}{x-1},$$

where  $\lambda$  is a free parameter. One then has to calculate,

$$\frac{1}{\pi} \int_{-1}^1 \frac{2(t'_0 - \lambda)dx}{[\lambda(x+1) - 2t'_0 - t(x-1)]} \rho_i^{\pm \text{box}}(w, t'(x)). \quad (143)$$

For the calculation of  $p_i^{\pm \text{cro}}(\bar{t}, t)$  and  $\text{Im}_w p_i^{\pm}(w, t)$  there is no discontinuity in  $t'_0$ . For  $p_i^{\pm \text{cro}}(\bar{t}, t)$ , one can transform the first term of (137) into an integral of the type (143). For the imaginary part the domain of definition of  $K(w, t')$  restricts the integration interval to  $[t'_0, +\infty]$ . There is a singularity at the lower limit in  $1/\sqrt{t' - t'_0}$  which we treat as above (see Eqs. (141) and (142)).

We have (see Eqs. (107), (135) and (137)),

$$p_i^{+ \text{box}}(w, t) = -p_i^{- \text{box}}(w, t), \quad p_i^{+ \text{cro}}(\bar{t}, t) = p_i^{- \text{cro}}(\bar{t}, t). \quad (144)$$

The proton-proton amplitude being a pure isospin one state (I=1), one has (see Eq. (87)),

$$\mathcal{M}^{I=1} = \sum_{i=1}^4 [p_i^{+ \text{box}}(w, t) + \text{Im} p_i^{+}(w, t) + 5p_i^{+ \text{cro}}(\bar{t}, t)] P_i. \quad (145)$$

We give below the formulae which express, for a given isospin state, the nucleon-nucleon helicities amplitudes  $\varphi_i$  in terms of the  $p_i$  amplitudes. One has [27],

$$\begin{aligned} \varphi_1 &= \frac{1+z}{2} (p_1 - 2mDp_2 + m^2D^2p_3) + \left( D - \frac{1-z}{2} \right) p_4, \\ \varphi_2 &= -\frac{1-z}{2} \left( \frac{E^2}{m^2}p_1 - \frac{2E^2}{m}p_2 + E^2p_3 + p_4 + \frac{k^2}{m^2}p_5 \right), \\ \varphi_3 &= \frac{1+z}{2} (p_1 - 2mDp_2 + m^2D^2p_3 + Dp_4), \\ \varphi_4 &= \frac{1-z}{2} \left( \frac{E^2}{m^2}p_1 - \frac{2E^2}{m}p_2 + E^2p_3 + p_4 - \frac{k^2}{m^2}p_5 \right), \\ \varphi_5 &= \frac{E\sqrt{1-z^2}}{2m} \left( -p_1 + \frac{2E^2}{m}p_2 - m^2Dp_3 - p_4 \right), \end{aligned} \quad (146)$$

where  $D = (E^2 + k^2)/m^2$  and  $z = \cos \theta$  (let us remember that in the center of mass of the nucleon-nucleon w-channel,  $w = 4E^2 = 4(k^2 + m^2)$  and  $t = -2k^2(1 - z)$ ). The Saclay amplitudes  $a$ ,  $b$ ,  $c$ ,  $d$  and  $e$  are given in terms of the  $\varphi_i$  amplitudes by the following expressions [36],

$$\begin{aligned} a &= \frac{1}{2} \left[ (\varphi_1 + \varphi_2 + \varphi_3 - \varphi_4)z - 4\varphi_5\sqrt{1-z^2} \right], \\ b &= \frac{1}{2} (\varphi_1 - \varphi_2 + \varphi_3 + \varphi_4), \\ c &= \frac{1}{2} (-\varphi_1 + \varphi_2 + \varphi_3 + \varphi_4), \\ d &= \frac{1}{2} (\varphi_1 + \varphi_2 - \varphi_3 + \varphi_4), \\ e &= -\frac{i}{2} \left[ (\varphi_1 + \varphi_2 + \varphi_3 - \varphi_4)\sqrt{1-z^2} + 4\varphi_5z \right]. \end{aligned} \quad (147)$$

## B. Nucleon pole contribution for Pseudo-vector coupling

For pseudo-vector pion-nucleon coupling, the  $A(B)_{1(2),PV}^\pm$  for the  $\pi N$  nucleon Born term are (see e.g. Eqs. (A.8.1) and (A.8.2) of Ref. [52]),

$$\begin{aligned} A_{1(2),PV}^+ &= \frac{g^2}{m}, \quad A_{1(2),PV}^- = 0, \\ B_{1(2),PV}^+ &= B_{1(2),PS}^+, \quad B_{1(2),PV}^- = B_{1(2),PS}^- - \frac{g^2}{2m^2}. \end{aligned} \quad (148)$$

One can then use Eqs. (104) and (105) to calculate the corresponding  $\rho_i^\pm$ . One recovers first the contribution for pseudo-scalar coupling from  $B_{1,PS}^\pm$   $B_{2,PS}^\pm$  given in the above section. There are further bubble (*bub*) diagram contributions arising from  $A_{1,PV}^+$   $A_{2,PV}^+$  and proportional to  $\left(\frac{g^2}{m}\right)^2$  and from  $B_{1,PV}^-$   $B_{2,PV}^-$  and proportional to  $\left(\frac{g^2}{2m^2}\right)^2$ . There are also triangle (*tri*) diagram contributions arising from  $B_{1,PV}^-$   $B_{2,PV}^-$  and proportional to  $\frac{g^2}{2m^2}$   $B_{1(2),PS}^-$ . One finds

$$\begin{aligned} \rho_1^{+bub}(t') &= \frac{g^4}{32\pi m^2} \sqrt{\frac{t' - 4\mu^2}{t'}}, \\ \rho_1^{+tri}(t') &= \frac{g^4}{16\pi} \sqrt{\frac{t' - 4\mu^2}{t'}} \frac{t' - 4\mu^2}{t' - 2\mu^2} I_2(t'), \\ \rho_2^{-tri}(t') &= -\frac{g^4}{128\pi m} \sqrt{\frac{t' - 4\mu^2}{t'}} \frac{t' - 4\mu^2}{t' - 4m^2} [I_0(t') - 3I_2(t')], \\ \rho_4^{-bub}(t') &= -\frac{t' - 4\mu^2}{48m^2} \rho_1^{+bub}(t'), \\ \rho_4^{-tri}(t') &= \frac{g^4}{256\pi m^2} \sqrt{\frac{t' - 4\mu^2}{t'}} (t' - 4\mu^2) [I_0(t') - I_2(t')]. \end{aligned} \quad (149)$$

In the above formulae (149)

$$I_{2n}(t') = \int_{-1}^{+1} \frac{u^{2n} du}{\alpha + \beta u}, \quad I_2(t') = \frac{\alpha}{\beta^2} [-2 + \alpha I_0(t')], \quad (150)$$

with  $\alpha = \mu^2 - t'/2$ . For  $t' < 4m^2$ ,  $\bar{\beta} = i\beta = i2[(m^2 - t'/4)(t'/4 - \mu^2)]^{1/2}$  and

$$I_0(t') = \frac{2}{\beta} \arctan \frac{\beta}{\alpha}. \quad (151)$$

For  $t' > 4m^2$ ,  $\bar{\beta} = \beta = 2[(t'/4 - m^2)(t'/4 - \mu^2)]^{1/2}$  and

$$I_0(t') = \frac{1}{\beta} \ln \left| \frac{\alpha + \beta}{\alpha - \beta} \right|. \quad (152)$$

The functions  $I_0(t')$  and  $I_2(t')$  are continuous at  $t' = 4m^2$  and

$$I_0(4m^2) = \frac{2}{\alpha}, \quad I_2(4m^2) = \frac{2}{3\alpha}. \quad (153)$$

Furthermore  $\rho_2^{-tri}(t')$  is also continuous at  $t' = 4m^2$ , with,

$$\lim_{t' \rightarrow 4m^2} \frac{I_0(t') - 3I_2(t')}{t' - 4m^2} = \frac{2(m^2 - \mu^2)}{(\mu^2 - 2m^2)^3}. \quad (154)$$

For  $t' \rightarrow \infty$  the functions  $I_{0,2}(t') \rightarrow (2/t') \ln(t'/m^2)$  and  $(t'/4 - \mu^2)[I_0(t') - I_2(t')] \rightarrow \text{constant}$ . It can then be seen from Eqs. (93) and (149) that the amplitudes  $p_1^{+tri}(t)$  and  $p_2^{-tri}(t)$  are convergent,  $p_1^{+bub}(t)$  and  $p_4^{-tri}(t)$  are logarithmically divergent and  $p_4^{-bub}(t)$  is linearly divergent. Introducing an upper limit of integration,  $t_M$ , in the integrals (93), one finds

$$p_1^{+bub}(t, t_M) = \frac{g^4}{32\pi^2 m^2} I_1(t, t_M), \quad (155)$$

$$p_4^{-bub}(t, t_M) = \frac{g^4}{1536\pi^2 m^4} I_4(t, t_M), \quad (156)$$

with

$$I_1(t, t_M) = I_1(0, t_M) + J_1(t, t_M), \quad (157)$$

$$I_1(0, t_M) = -2X(t_M) - I_{\ln}(X(t_M), 1), \quad (158)$$

$$J_1(t, t_M) = 2X(t_M) + X(t)I_{\ln}(X(t_M), X(t)), \quad (159)$$

$$X(t) = \sqrt{1 - \frac{4\mu^2}{t}}, \quad I_{\ln}(Y, Z) = \ln \left| \frac{Y - Z}{Y + Z} \right|, \quad (160)$$

$$I_4(t, t_M) = I_4(0, t_M) + J_4^1(t, t_M) + J_4^2(t, t_M), \quad (161)$$

$$I_4(0, t_M) = t_M X^5(t_M) - 6(\mu^2/t_M)J_4^1(t_M, t_M), \quad (162)$$

$$J_4^1(t, t_M) = -t[(2/3)X^3(t_M) - I_1(0, t_M)], \quad (163)$$

$$J_4^2(t, t_M) = t[(2/3)X^3(t_M) + X^2(t)J_1(t, t_M)]. \quad (164)$$

The logarithmic divergence of  $p_1^{+bub}(t)$  is seen in Eq. (159) and the linear divergence of  $p_4^{-bub}(t)$  in Eq. (162).

The  $\rho_1^{+bub}(t')$ ,  $\rho_1^{+tri}(t')$  contributions and those of  $\rho_2^{-tri}(t')$ ,  $\rho_4^{-bub(tri)}(t')$  can be interpreted as coming from the correlated  $2\pi$ -exchange in the S-wave ( $\sigma$  or  $f_0(600)$  exchange) and in the P-wave ( $\rho$  exchange), respectively (see Eqs. (2.29), (2.30), (2.31) of Ref. [27] and Eqs. (2.12), (2.13) of Ref. [25]). However, here there is no contribution to  $\rho_1^-$  as  $A^- = 0$ .

It is interesting to examine the box- and crossed-diagram contributions to the bubble and triangle diagrams arising from the pseudo-vector coupling case. Performing a similar reduction to that of  $P_{PV}$  (see Eq. (26) in section II.B) one can write the direct and crossed,  $T_{s_1}^{\alpha\beta}\pi N$  amplitudes as

$$T_{s_1}^{\alpha\beta} = \tau_\alpha^1 \tau_\beta^1 [A1^1 + \gamma^1 \cdot \mathbf{Q}(B_{s_1} - B_r)], \quad (165)$$

$$T_{\bar{s}_1}^{\alpha\beta} = \tau_\beta^1 \tau_\alpha^1 [A1^1 - \gamma^1 \cdot \mathbf{Q}(B_{\bar{s}_1} - B_r)]. \quad (166)$$

Here the Pauli matrices  $\tau_{\alpha(\beta)}^1$  represent the isospin coupling of the pion field  $\pi_{\alpha(\beta)}$  to the nucleon 1. In Eqs. (165) and (166),

$$A = \frac{g^2}{2m}, \quad B_r = \frac{g^2}{4m}, \quad B_s = \frac{g^2}{m^2 - s}. \quad (167)$$

Note that

$$\sum_{\alpha, \beta=1,2,3} \tau_{\alpha}^1 \tau_{\beta}^1 \tau_{\alpha}^2 \tau_{\beta}^2 = \sum_{\alpha, \beta} (\delta_{\alpha\beta} + i\epsilon_{\alpha\beta\gamma} \tau_{\gamma}^1) (\delta_{\alpha\beta} + i\epsilon_{\alpha\beta\gamma} \tau_{\gamma}^2) = 3 - 2\boldsymbol{\tau}^1 \cdot \boldsymbol{\tau}^2. \quad (168)$$

The  $2\pi$ -exchange box diagram contribution arises from

$$\begin{aligned} T_{box} &= T_{s_1}^{\alpha\beta} T_{s_2}^{\alpha\beta} + T_{\bar{s}_1}^{\alpha\beta} T_{\bar{s}_2}^{\alpha\beta} \\ &= (3 - 2\boldsymbol{\tau}^1 \cdot \boldsymbol{\tau}^2) \{ 2A^2 1^1 1^2 + (B_{s_1} - B_{\bar{s}_1}) A (1^2 \boldsymbol{\gamma}^1 \cdot \mathbf{Q} + 1^1 \boldsymbol{\gamma}^2 \cdot \mathbf{Q}) \\ &\quad + 2 [B_{s_1} B_{s_2} - B_r (B_{s_1} + B_{s_2}) + B_r^2] \boldsymbol{\gamma}^1 \cdot \mathbf{Q} \boldsymbol{\gamma}^2 \cdot \mathbf{Q} \}. \end{aligned} \quad (169)$$

The crossed diagram contribution is,

$$\begin{aligned} T_{cro} &= T_{s_1}^{\alpha\beta} T_{\bar{s}_2}^{\alpha\beta} + T_{\bar{s}_1}^{\alpha\beta} T_{s_2}^{\alpha\beta} \\ &= (3 + 2\boldsymbol{\tau}^1 \cdot \boldsymbol{\tau}^2) \{ 2A^2 1^1 1^2 + (B_{s_1} - B_{\bar{s}_1}) A (1^2 \boldsymbol{\gamma}^1 \cdot \mathbf{Q} + 1^1 \boldsymbol{\gamma}^2 \cdot \mathbf{Q}) \\ &\quad - 2 [B_{s_1} B_{\bar{s}_2} - B_r (B_{s_1} + B_{\bar{s}_2}) + B_r^2] \boldsymbol{\gamma}^1 \cdot \mathbf{Q} \boldsymbol{\gamma}^2 \cdot \mathbf{Q} \}. \end{aligned} \quad (170)$$

In Eqs. (169) and (170) the terms  $B_{s_1} B_{s_2}$  and  $B_{s_1} B_{\bar{s}_2}$  correspond to the  $2\pi$ -exchange nucleon pole contribution for pseudo-scalar coupling. For the bubble and triangle diagram contributions, use of Eqs. (104) and (105) leads to

$$\begin{aligned} \rho_{1\ box}^{\pm bub}(t') &= \pm \rho_{1\ cro}^{\pm bub}(t') = \pm \frac{1}{2} \rho_1^{+bub}(t'), \\ \rho_{1\ box}^{\pm tri}(t') &= \pm \rho_{1\ cro}^{\pm tri}(t') = \pm \frac{1}{2} \rho_1^{+tri}(t'), \\ \rho_{2\ box}^{\pm tri}(t') &= \mp \rho_{2\ cro}^{\pm tri}(t') = \mp \frac{1}{2} \rho_2^{-tri}(t'), \\ \rho_{4\ box}^{\pm bub}(t') &= \mp \rho_{4\ cro}^{\pm bub}(t') = \mp \frac{1}{2} \rho_4^{-bub}(t'), \\ \rho_{4\ box}^{\pm tri}(t') &= \mp \rho_{4\ cro}^{\pm tri}(t') = \mp \frac{1}{2} \rho_4^{-tri}(t'). \end{aligned} \quad (171)$$

It can be seen that the total  $\rho_i^{\pm bub(tri)}(t') + \rho_i^{\pm bub(tri)}(t')$  from the above formulae (171) are in agreement with the formulae (149) calculated from Eqs. (148). Formulae (171) satisfy the relations of Eq. (135) between the box and crossed  $\rho_i$ .

### C. Comparison with Feynman diagram calculation

We have checked, at different energies and angles, that the Saclay amplitudes given by Eq. (147) for both box and crossed diagrams for pseudo-scalar coupling calculated in Section II-A from the Feynman diagram expressions with no form factor ( $\Lambda \rightarrow \infty$ ) are in agreement with the corresponding dispersion relation results Eq. (136), Eq. (137) and Eq. (138). We found that the short range contribution of the crossed diagram coming from the term containing  $a_i^{\pm}(w', 4m^2 - w - w')$  in Eq. (93) is crucial for the agreement. Numerical comparisons will be shown in the next section.

For the pseudo-vector coupling, the comparison of the bubble and triangle contributions Eq. (149) is less straightforward due to the divergence of some of these terms when integrated on  $t'$  in the dispersion relation or of the corresponding terms in the limit of  $\Lambda \rightarrow \infty$  in the Feynman method. The results of both approaches for the convergent invariant amplitudes  $p_1^{+tri}(t)$  and  $p_2^{-tri}(t)$  (see Eqs. (149)) compare well. The logarithmically divergent  $p_1^{+bub}(t)$  and  $p_4^{-tri}(t)$  require one subtraction and a comparison can be made with the  $dp_1^{+bub}(t)/dt$  and  $dp_4^{-tri}(t)/dt$ . For the linearly divergent  $p_4^{-bub}(t)$  the second derivative,  $d^2p_4^{-bub}(t)/dt^2$ , converges and can be compared with the Feynman calculation.

To obtain these amplitudes in the Feynman calculation the amplitudes  $p_4$  and  $p_1$  are extracted by solving for them from Eqs. (146) and (147) thus removing the explicit dependence on the cosine of the scattering angle,  $z$ . Then the derivatives with respect to  $z$  are essentially the same as the derivatives with respect to  $t$  in the case of the dispersion relations allowing a direct numerical comparison. Since this process requires numerical derivatives and a calculation for large  $\Lambda$  it is more difficult, but a good agreement is obtained.

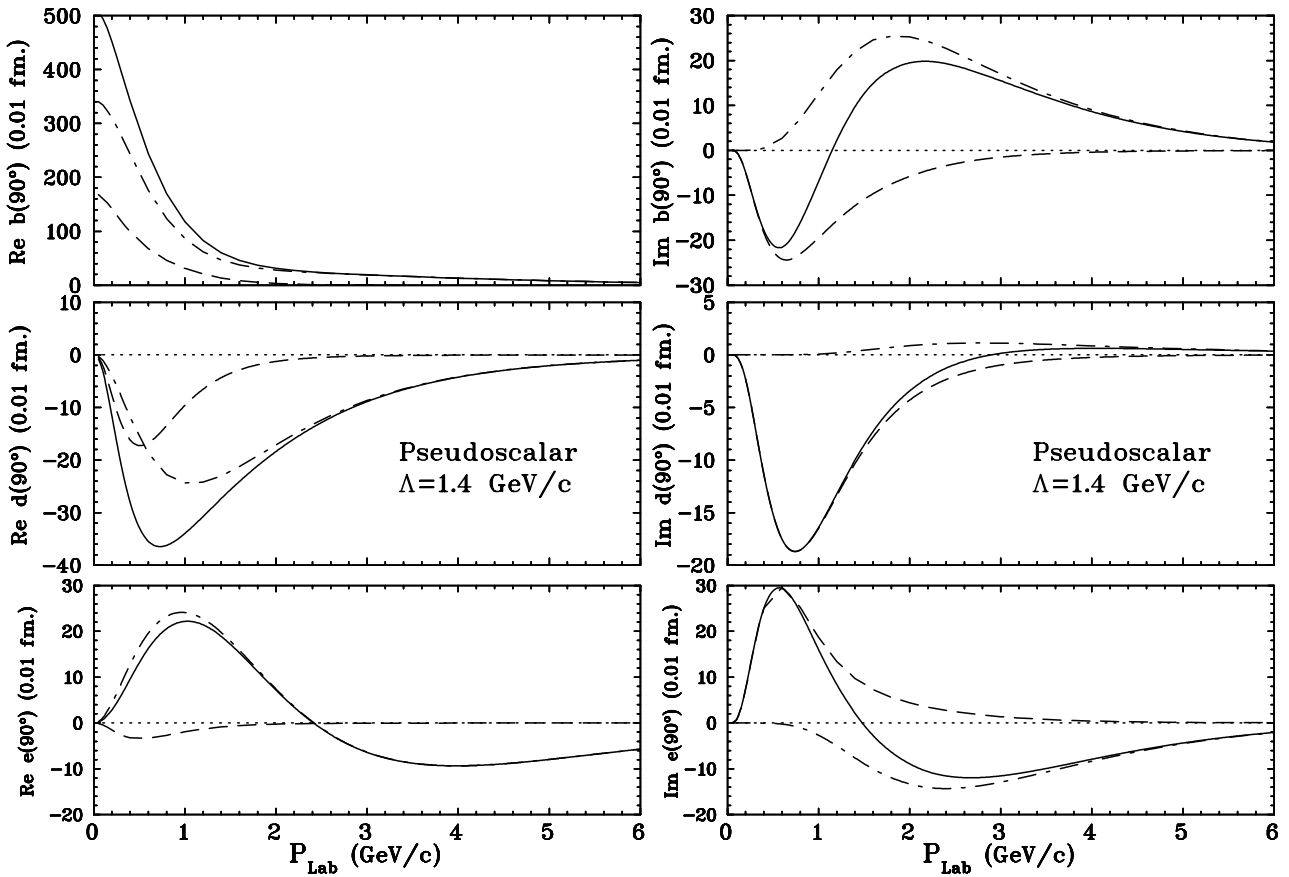


FIG. 6: Contributions to the real (left) and imaginary (right) parts of the amplitudes  $b$ ,  $d$  and  $e$  as a function of energy for pseudo-scalar coupling. The dashed line corresponds to the box, the dashed-dot line to the crossed-pion diagram and the solid line to their sum.

## VI. RESULTS AND DISCUSSION

Test calculations were made with and without the antiproton poles ( $p_0 = -E$ ). At low values of  $P_{Lab}$  or for large  $\Lambda$  they give significant contributions and are essential to get agreement with the dispersion relation results. However, for realistic values of  $\Lambda$  at higher energies they become unimportant and can be neglected.

Figure 6 shows the behavior of the real and imaginary parts of the amplitudes as a function of incident momentum

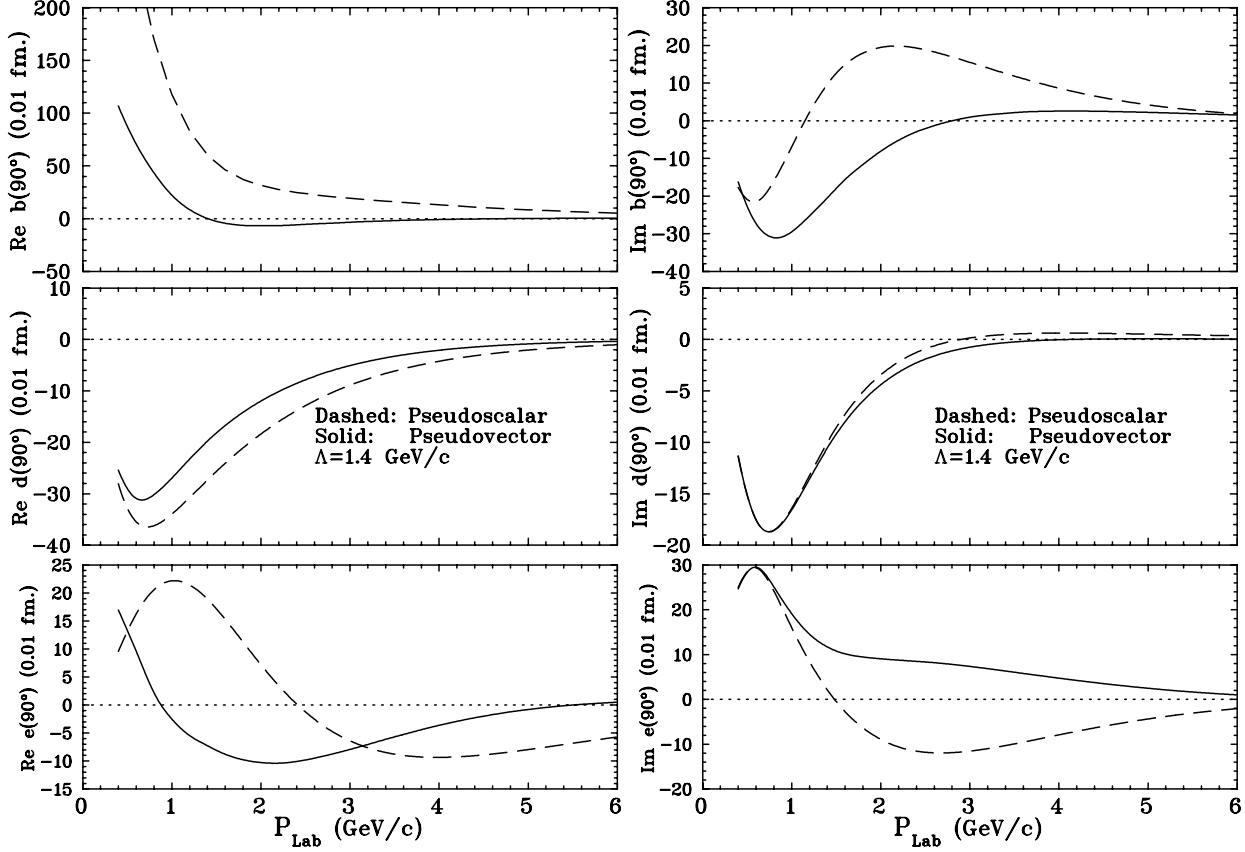


FIG. 7: Comparison of the real (left) and imaginary (right) parts of the amplitudes  $b$ ,  $d$  and  $e$  corresponding to the pseudo-scalar and pseudo-vector couplings. The dashed curve represents the PS and the solid curve the PV.

for the pseudo-scalar coupling. For the crossed-pion diagram only terms with a single nucleon or pion on shell and the principal value integral on  $q_0$  survive. That is to say, only the contributions from the  $q_0$  integral need to be treated specially, the rest of the indicated integrals have no singularities. For the box diagram, in addition to the two contributions just mentioned, the diagram in which two nucleons are on shell also gives a real contribution (in the form we are looking at now, it becomes an imaginary contribution to the amplitude after application of the factor of  $i$  to be consistent with the dispersion relation approach). That is, the integral on the magnitude of the three-momentum also has a  $\delta$ -function part which contributes.

In figure 6 (imaginary part) we see that the principal-value part of the integral goes rapidly to zero for the crossed diagram as the momentum drops below 500 MeV/c. This behavior can be traced to the form factor and its dependence on  $q_0$ . For low energy the form factor becomes independent of  $q_0$ , since the pole moves far from the real axis. Since it is the only pole off of the real axis the integrand limits to a function with only poles on the real axis and hence contains only the  $\delta$ -function parts.

The imaginary part of the box contains both the principal value and double pole contribution. At low energies the real parts of the amplitudes are dominated by the term with two nucleons on shell. By 2 GeV/c that situation has been reversed with the crossed-pion principal value dominating.

Figure 7 compares the results for the pseudo-scalar and pseudo-vector couplings. One sees that the real part of the Sackay amplitude  $b$  is very large for the PS coupling but is greatly reduced for PV coupling. The  $d$  amplitude shows only a modest difference between PS and PV coupling while the  $e$  amplitude is again significantly modified. We note that the  $b$  amplitude is a mixture of central and spin-spin character, the  $d$  amplitude is of tensor character and the  $e$  amplitude is of spin-orbit character [17].

Figures 8 and 9 show a comparison of the box and crossed-pion contributions. It is readily seen that the crossed-pion diagram dominates at high energy. This result can be traced back to the relative ability of the two diagrams to

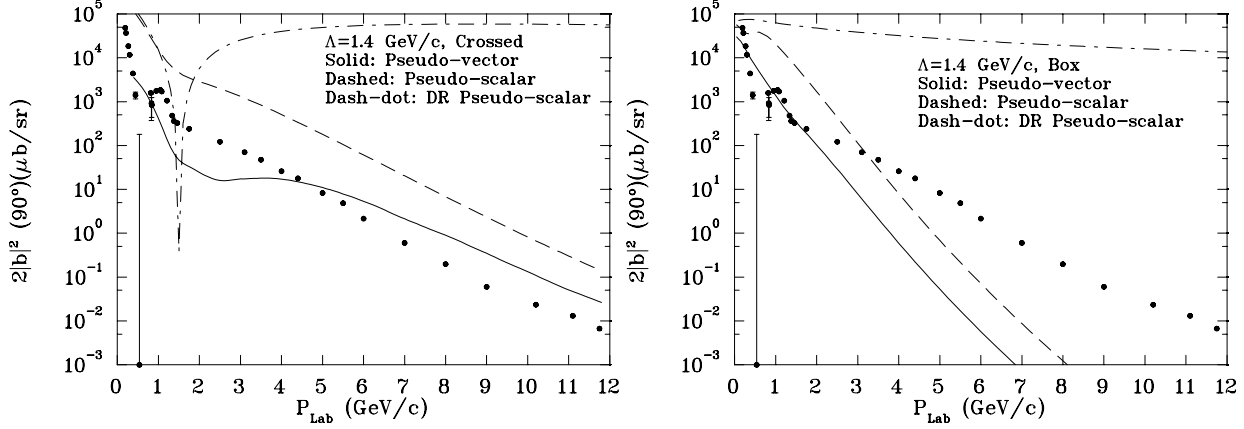


FIG. 8: Results for the crossed (left) and box diagram (right) for the  $b$  amplitude. The dash-dot curves show the results of the dispersion relation calculation, equivalent to the Feynman calculation for  $\Lambda \rightarrow \infty$ .

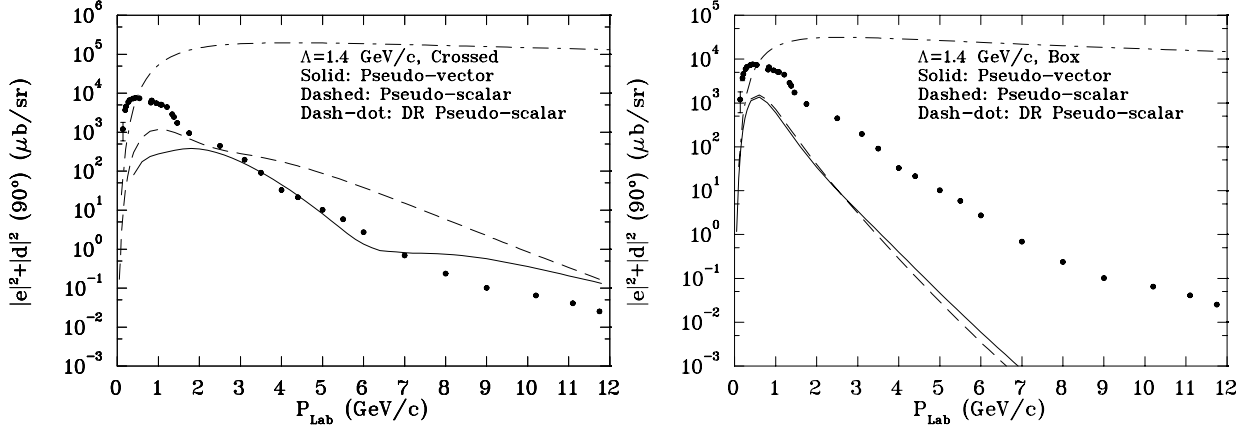


FIG. 9: Results for the crossed (left) and box diagram (right) for the  $d$  and  $e$  amplitudes. The curves have the same meaning as in Fig. 8.

transfer energy and momentum. Because factors of momentum transfer in the numerator cancel the decrease coming from the propagators, the integrand without form factors does not fall off with increasing momentum transfer so that the decrease in cross section is mainly due to the form factors. Since the form factor falls off with increasing pion momentum in the center of mass of the nucleon, one can see that for the box diagram with the four-vector  $q$  connecting vertices with  $(E, \mathbf{k})$  and  $(E, -\mathbf{k})$  both momenta in the respective centers of momentum cannot be zero (or even small) at the same time. The crossed diagram does not suffer from this contradiction since  $\mathbf{q}$  connects  $-\mathbf{k}$  and  $\mathbf{k}'$  and, for some value of the 4-vector,  $q$ , there is a chance to minimize the momenta at both vertices. We now look at the behavior of the form factor chosen for these calculations.

The crucial element for the understanding of the behavior of the box and crossed diagrams is the argument  $Z^2$  in Eq. (84). Since one nucleon is always on-shell we can write  $Z^2$  as

$$Z^2 = \frac{(a \cdot b)^2}{m^2} - b^2, \quad (172)$$

where  $a = \pm k$  or  $\pm k'$  and  $b = q$  or  $q'$ .

The order of magnitude of  $\tilde{q} = |\mathbf{q}|$  will be the same as  $|\mathbf{k}|$  since  $\tilde{q}$  cannot be taken as small to maximize the integrand because of the powers of  $\tilde{q}$  in the numerator. For values of momenta greater than the mass of the nucleon, the first term,  $(a \cdot b)^2$ , will dominate so we need only consider the size of that term to obtain some sense of the behavior of the form factor. Out-of-plane values of  $\mathbf{q}$  (in the  $y$  direction in the system we are using) only increase  $Z^2$  so consider



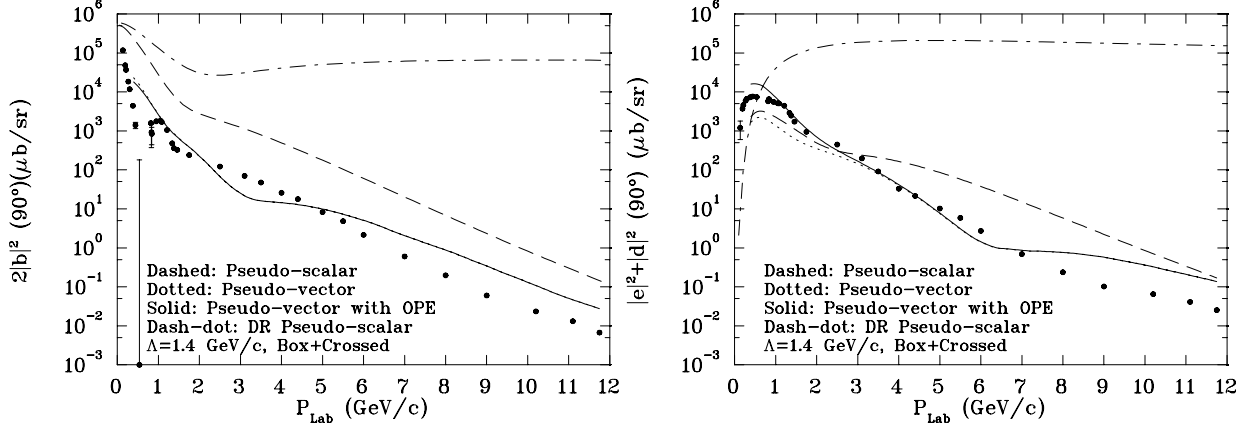


FIG. 10: Results of the sum of the crossed and box diagrams for  $2|b|^2$  (left) and  $|d|^2 + |e|^2$  (right). The dash-dot curves show the results of the dispersion relation calculation, equivalent to the Feynman calculation for  $\Lambda \rightarrow \infty$ .

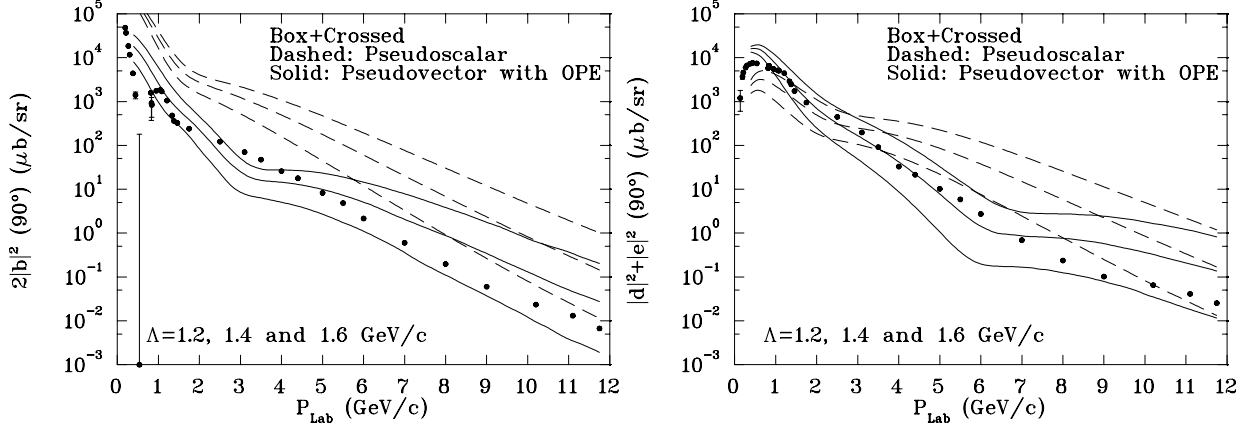


FIG. 11: Comparison of the data for  $2|b|^2$  (left) and  $|d|^2 + |e|^2$  (right) with the results of the sum of the crossed and box diagrams for different values of  $\Lambda$ . Increasing cross sections correspond to increasing values of  $\Lambda$ .

$q_y = 0$ . Let  $x$  be the cosine between the incident direction  $\mathbf{k}$  and the vector  $\mathbf{q}$  and consider the pole at  $q_0 = \omega$  in an extreme relativistic limit  $E \rightarrow \tilde{k}$  ( $\tilde{k} = |\mathbf{k}|$ ) and  $\omega \rightarrow \tilde{q}$ .

It is useful to look for the minimum in the four values of  $Z^2$  in order to maximize the form factor. Corresponding to the four factors in Eq. (85) we have (neglecting the second term in  $Z^2$ ) the following four values for  $a \cdot b$  for the box diagram;

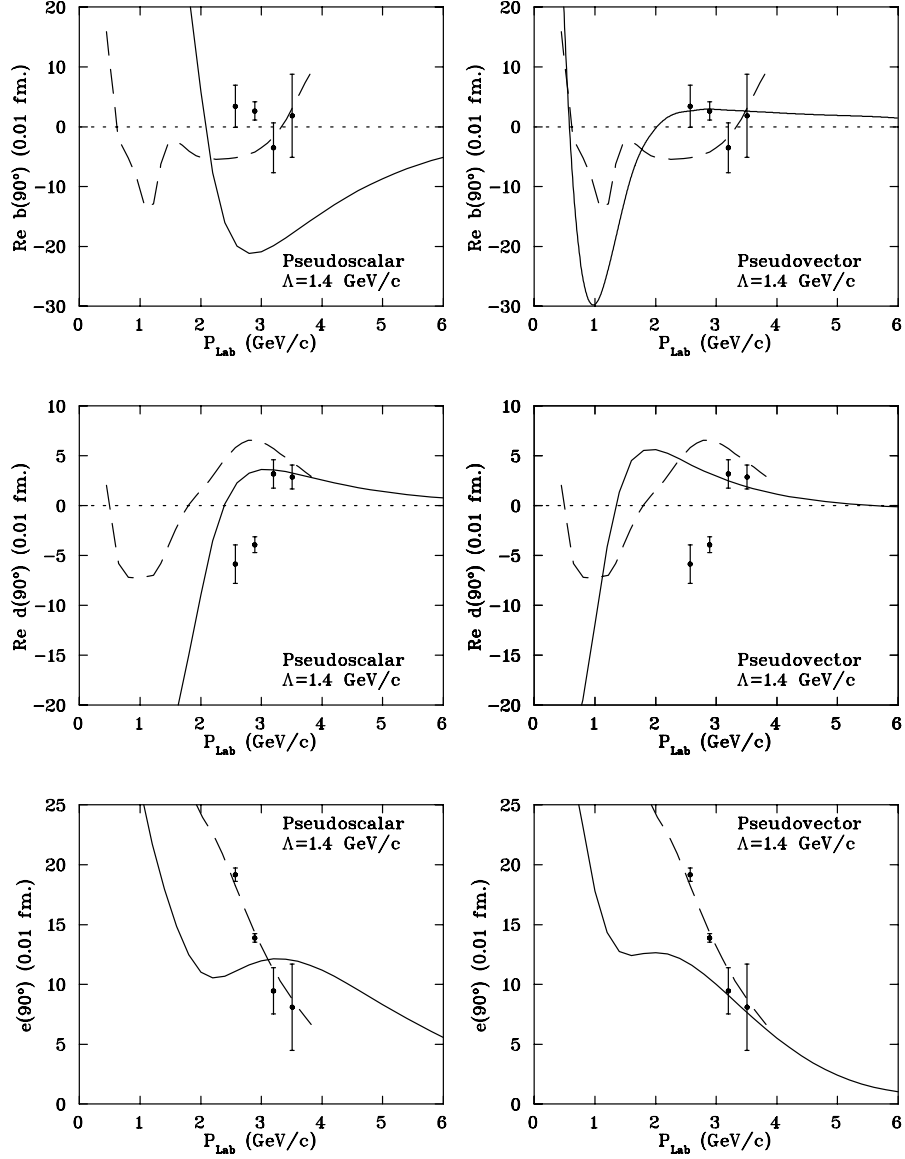


FIG. 12: Comparison of the real parts of the calculated PS (left) and PV (right)  $b$ ,  $d$  and  $e$  amplitudes (solid lines) with the results of SAID [57] (dashed lines) and those obtained by Bystricky et al. (points) [58]. The phase has been chosen such that the amplitude  $e$  is real.

$$1) E\omega - \mathbf{k} \cdot \mathbf{q} \rightarrow \tilde{k}\tilde{q}(1-x); \quad 2) E\omega + \mathbf{k} \cdot \mathbf{q} \rightarrow \tilde{k}\tilde{q}(1+x);$$

$$3) E\omega - \mathbf{k}' \cdot \mathbf{q}' \rightarrow \tilde{k}[\tilde{q}(1 - \sqrt{1-x^2}) + \tilde{k}]; \quad 4) E\omega + \mathbf{k}' \cdot \mathbf{q}' \rightarrow \tilde{k}[\tilde{q}(1 + \sqrt{1-x^2}) - \tilde{k}]. \quad (173)$$

Since the first and second vertices involve the sum and difference of the same quantities, they cannot both be small at the same time. The form factor being an even function of  $x$ , there is an extremum at  $x = 0$  and, in fact, it is a

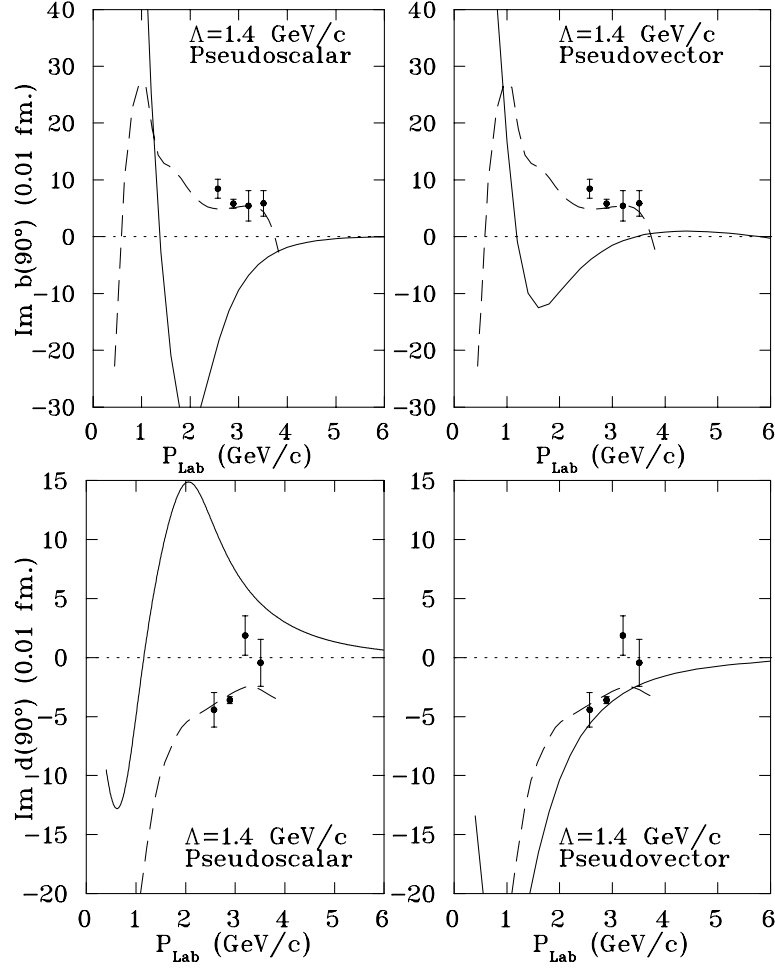


FIG. 13: As in Fig. 12 but for the imaginary part of the  $b$  and  $d$  amplitudes.

maximum. If we choose  $x = 0$  and the fourth value of  $a \cdot b$  to be zero with  $\tilde{q} = \frac{1}{2}\tilde{k}$  then, in this limit

$$\mathcal{F}_{box}^{\max} \rightarrow \frac{1}{\left(1 + \frac{\tilde{k}^4}{4m^2\Lambda^2}\right)^4} \frac{1}{\left(1 + \frac{\tilde{k}^4}{m^2\Lambda^2}\right)^2}. \quad (174)$$

We can apply the same considerations for the crossed-pion graph from Eq (86). The values of  $a \cdot b$  at the four vertices are

$$\begin{aligned} &1) E\omega - \mathbf{k} \cdot \mathbf{q}' \rightarrow \tilde{k}\tilde{q}(1-x) - \tilde{k}^2; \quad 2) E\omega + \mathbf{k} \cdot \mathbf{q} \rightarrow \tilde{k}\tilde{q}(1+x); \\ &3) E\omega - \mathbf{k}' \cdot \mathbf{q} \rightarrow \tilde{k}\tilde{q}(1 - \sqrt{1-x^2}); \quad 4) E\omega + \mathbf{k}' \cdot \mathbf{q}' \rightarrow \tilde{k}\tilde{q}(1 + \sqrt{1-x^2}) - \tilde{k}^2. \end{aligned} \quad (175)$$

It is possible to find values of  $\tilde{q}$  and  $x$  such that any of the values of  $Z^2$  is zeroed, unlike the case of the box diagram where the third value can never be zero. For example, one could take  $x = -1$  and  $\tilde{q} = \frac{1}{2}\tilde{k}$  to set the first and second values of  $Z^2$  to zero. The maximum comes about, however, if we take the first and fourth values of  $a \cdot b$  to be zero which leads to

$$\tilde{q} = (2 - \sqrt{2})\tilde{k}; \quad x = -1/\sqrt{2}. \quad (176)$$

The second and third values of  $a \cdot b$  become

$$(3 - 2\sqrt{2})\tilde{k}^2 \approx 0.1716\tilde{k}^2, \quad (177)$$

which is much smaller than what one was able to achieve in the case of the box diagram. The form factor is then

$$\mathcal{F}_{crossed}^{\max} \rightarrow \frac{1}{\left[1 + \left(\frac{0.1716\tilde{k}^2}{m\Lambda}\right)^2\right]^4}. \quad (178)$$

Thus, not only is it possible to make two of the arguments zero at the same time but the other two are relatively small also. Numerical studies of the relative sizes of the form factors alone confirm that the values of the maximum of the crossed form factor occurs at the values given by Eq. (176). While it is necessary to go to very high energy to justify the ultra-relativistic limit used above for illustration, at  $P_{Lab}=5.5$  GeV/c typical values of the crossed diagram form factor are more than two orders of magnitude larger than that for the box diagram.

Since the crossed-pion form factor peaks at definite values of  $\mathbf{q}$  and  $x$  at high energies, analytical predictions of the relative size of the different amplitudes can be made. From these values we find for the Saclay amplitudes, in the very high-energy limit

$$e = -2b; \quad d = 0, \quad (179)$$

which was verified by a calculation at  $P_{Lab} = 46$  GeV/c. These values lead to a value of  $C_{NN}$  which is again 1/3. In the energy range where we compare with data we are far from this limit, however.

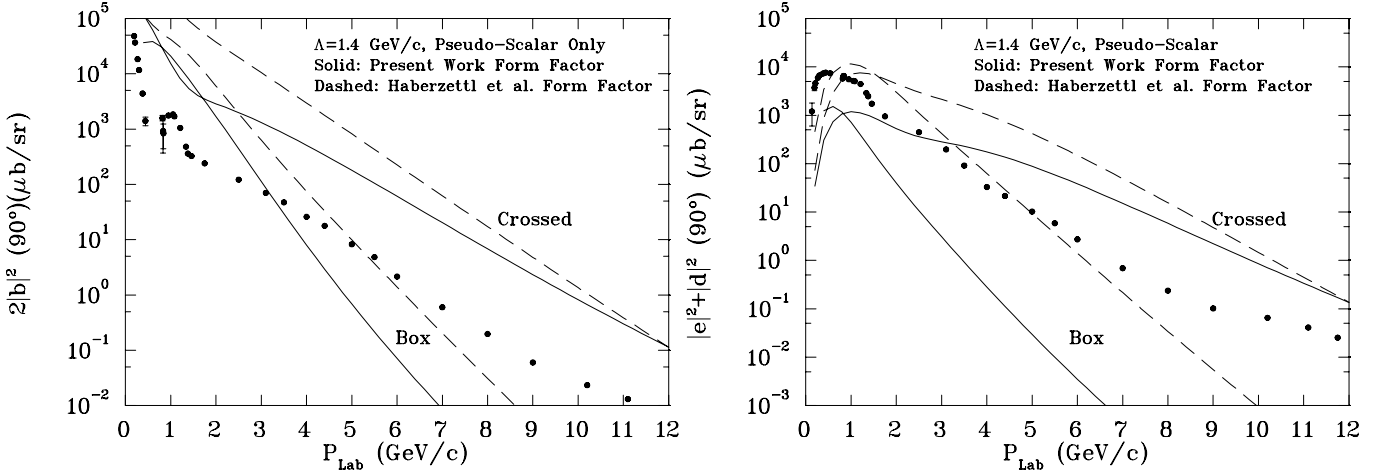


FIG. 14: Comparison of calculations using  $Z^2$  as the variable in a dipole form factor with that of Eq. (180) from Haberzettl et al. [43]. No attempt has been made to make the range the same in the two calculations and this figure gives only the PS contribution. The graph shows that the slopes of the calculations with the different form factors are similar and in both cases the box diagram contribution falls off much more rapidly than that of the crossed diagram.

We see that the values of the spin separated cross sections shown in Fig. 11 indicate a preference for the PV coupling and values of  $\Lambda$  in the range 1.2 to 1.4. Since  $\Lambda$  has been limited from other sources (see Section IV A), the agreement is obtained in a nearly parameter free manner.

Some experimental values of the Saclay amplitudes are known at high enough energy that unitarity corrections can be expected to be small enough that they can be compared with the present calculation. Arndt et al. [57] give amplitudes up to  $P_{Lab} = 3.82$  GeV/c and Bystricky et al. [58] present several single energy values. Ghahramany and Forozani [59] found values of the amplitudes at two energies in reasonable agreement with Refs. [57] and [58]. Figure 12 shows a comparison of the present calculation with the SAID values (broken line) and the Bystricky et al. points. The agreement for the pseudo-vector coupling is seen to be considerably better than the pseudo-scalar one and gives a reasonable representation of the data except for the imaginary part of  $b$ .

One may ask if the difference in fall-off of the crossed and box diagrams is a general result of the kinematics or if it depends on the particular form of the variable  $Z^2$  used in the form factor. To attempt to give a partial answer to this question we have calculated the pseudo-scalar result for the crossed diagram with a different, though superficially similar, variable. Haberzettl et al. [43] use a variable which is of the form

$$W^2(p_1, p_2, p_3) = \frac{(p_1^2 - m_1^2)^2 + (p_2^2 - m_2^2)^2 + (p_3^2 - m_3^2)^2}{4m^2} \quad (180)$$

where we have chosen the normalization such that the limit for large values of the invariant masses the limit matches that of Eq. (80). Figure 14 shows the comparison of the two calculations and one sees that the fall-off for this variable is very similar to the presently used form factor. The rise at small momenta is at least partially due to the contribution of the principal value integral since the pole in the complex plane does not move far from the real axis as the energy goes to zero so that causality is not respected in that limit.

It is useful to examine the decrease of the cross section with increasing energy. The prediction of slope of Brodsky and Farrar [18] (see Fig. 1) based on counting of internal propagators and our calculation of  $2|b|^2$  are very similar. The high energy limit of a form factor has been compared with the picture of the propagators between interacting constituents by the authors of Ref. [60] for the case of scattering from nuclear constituents. The two-pion-exchange diagram may be able to provide a bridge between the low and high-energy points of view.

The present result bears directly on the question of the energy regime where the transition from a color singlet hadronic exchange to a quark-gluon basis might reasonably take place. This, in turn, may impact the question of color transparency (see, for example Jain et al. [61]). If the exchange of color singlets (pions in this case) continues to be important through 12 GeV/c it might negate the basis for color transparency (dominance of quark-gluon exchange) in the moderate energy range  $P_{Lab} \leq 12$  GeV/c. This is the entire range covered in the color transparency experiments of Carroll et al. [62]. However, it may be that, even if color singlet exchange continues to be very important for elastic scattering, quark-gluon exchange might dominate the inelastic processes.

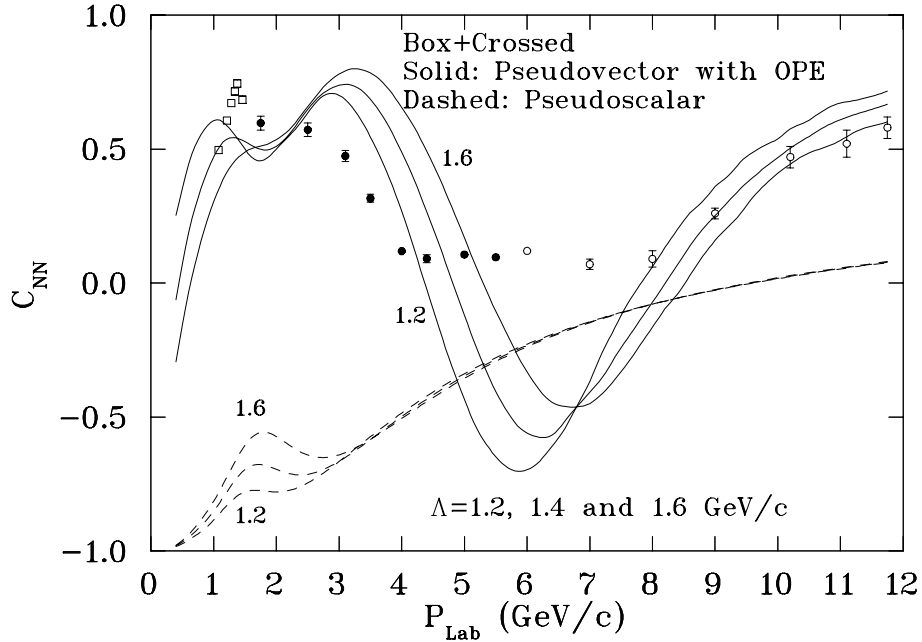


FIG. 15: Comparison of the result for the spin-correlation observable  $C_{NN}$  for the PS and PV couplings for three values of  $\Lambda$ . Data are: Squares, Bhatia et al. [2], Filled circles, Lin et al. [1], Open circles, Crosbie et al. [3].

The comparison with the spin transfer observable  $C_{NN}$  is given in Fig. 15 for several values of  $\Lambda$ . For the pseudo-vector choice of coupling it is seen that the qualitative features are reproduced. One, in fact, needs a mechanism (or several mechanisms) with considerable structure in order to reproduce the data. The plateau in the data from 4 to 8 GeV/c is not found but there is a minimum in the calculation in this region.

## VII. SUMMARY AND CONCLUSIONS

We have calculated the contribution of the box and crossed two-pion-exchange diagrams to proton-proton scattering at  $90^\circ_{c.m.}$  for laboratory momenta up to 12 GeV/c. The cases of both pure pseudo-scalar and pure pseudo-vector pion-nucleon coupling are treated.

We assume that the interaction of the pion is with the valence quarks within the nucleons and use an effective field theory obeying Feynman rules to describe the composite system. At each pion-nucleon-interaction vertex we introduce a relativistic Lorentz-invariant form factor. These form factors are related to the convolution of the nucleon and pion sizes and represent the pion source distribution based on the quark structure of the hadronic cores and explicitly introduce an interaction range of this size. These form factors are functions of the four-momenta of the exchanged pions and scattering nucleons. One can use any two of the three momenta which converge at a given vertex to calculate the function so that the dependence on the nucleon and pion momenta displays a high degree of symmetry. This behavior can be traced to the fact that the basic scalar on which the form factors depend can be written as the square of the four-dimensional cross product of any two of the three four-vectors.

While we believe the form factors that we introduce are quite reasonable, we make no claim as to their uniqueness. However, there exist a set of conditions, based on short reaction time, causality etc., that any relativistic Lorentz invariant form factor should satisfy. Our form factors obey these rules, but other form factors used by some authors do not.

As a check of the calculation, we compare the two-pion-exchange Feynman-diagram amplitudes for both pseudo-scalar and pseudo-vector coupling calculated with point-like nucleons with those obtained from the dispersion relation approach and find agreement. The antiproton poles in the Feynman calculations are essential for the comparison but for a more realistic calculation with a finite value of the form-factor range,  $\Lambda$ , they are unimportant. While performing this study, we found it essential to include a contribution of the crossed diagram which was neglected in the dispersion-relation calculations of the two-pion-exchange Paris potential because of its very short range.

The numerical technique for calculating the 4-dimensional Feynman integrals, taking into account multiple poles is presented. Standard transformation methods are not always applicable in the presence of form factors.

In the Feynman diagram calculations, using the form factors constrained by the valence quark distribution, comparison with experimental data favors the pseudo-vector coupling over the pseudo-scalar one. This is seen in the comparison with the magnitude of the spin-separated cross sections, in the agreement with amplitudes extracted up to 4 GeV/c and in the spin transfer parameter  $C_{NN}$ , although in this later case it is only the general behavior which is correctly given.

The exchange of one pion is important only at momentum less than  $P_{Lab}=1$  GeV/c. While the strengths of the box and crossed diagrams for the exchange of two pions are comparable for laboratory momenta below 2 GeV/c, for larger momenta the crossed diagram dominates, mainly due to the mathematical structure of the form factors and to the fact that the kinematics of the crossed diagram allows a repartition of momenta at the vertices in a favorable manner. An important contribution arises from the principal-value contribution of the integrals which is non-zero when form factors are included.

While here we compare only with the extracted spin-separated cross sections at  $90^\circ_{c.m.}$ , our calculation can be extended to all scattering angles. Further studies such as unitarity corrections can be considered.

To conclude, we have shown that the two-pion exchange plays a significant role in proton-proton scattering even up to  $P_{Lab}=12$  GeV/c. This result suggests that the importance of the exchange of color singlets in elastic scattering may extend to higher energies than expected.

### Acknowledgments

We thank Helmut Haberzettl for a useful conversation regarding causality, Henri Zytnicki for providing support for this project with his work and Jean-Pierre Dedonder and R. Vinh Mau for helpful comments on the manuscript.

This work was supported by the National Science Foundation under contract PHY-0099729.

## Appendices

## APPENDIX A: PROJECTION ONTO THE SACLAY AMPLITUDES

The Saclay amplitudes [36] are defined by the equation

$$M(\mathbf{k}_f, \mathbf{k}_i) = \frac{1}{2}[(a+b) + (a-b)\boldsymbol{\sigma}_1 \cdot \mathbf{n}\boldsymbol{\sigma}_2 \cdot \mathbf{n} + (c+d)\boldsymbol{\sigma}_1 \cdot \mathbf{m}\boldsymbol{\sigma}_2 \cdot \mathbf{m}, \\ + (c-d)\boldsymbol{\sigma}_1 \cdot \mathbf{l}\boldsymbol{\sigma}_2 \cdot \mathbf{l} + e(\boldsymbol{\sigma}_1 + \boldsymbol{\sigma}_2) \cdot \mathbf{n}] \quad (\text{A1})$$

where the center-of-mass basis vectors are:

$$\mathbf{l} = \frac{\mathbf{k}_f + \mathbf{k}_i}{|\mathbf{k}_f + \mathbf{k}_i|}, \quad \mathbf{m} = \frac{\mathbf{k}_f - \mathbf{k}_i}{|\mathbf{k}_f - \mathbf{k}_i|}, \quad \mathbf{n} = \frac{\mathbf{k}_i \times \mathbf{k}_f}{|\mathbf{k}_i \times \mathbf{k}_f|}. \quad (\text{A2})$$

Observables at  $90^\circ$  are

$$\sigma = \frac{1}{2}(2|b|^2 + |d|^2 + |e|^2); \quad \sigma C_{NN} = \frac{1}{2}(-2|b|^2 + |d|^2 + |e|^2); \quad (\text{A3})$$

$$\sigma D_{NN} = \frac{1}{2}(-|d|^2 + |e|^2) = \sigma K_{NN}; \quad \sigma C_{MMMM} = \frac{1}{2}(2|b|^2 + |d|^2 - |e|^2). \quad (\text{A4})$$

The expressions for the amplitudes in terms of the singlet-triplet matrix elements are:

$$a = \frac{1}{2}(M_{11} + M_{00} - M_{1-1}); \quad b = \frac{1}{2}(M_{11} + M_{ss} + M_{1-1}); \quad (\text{A5})$$

$$c = \frac{1}{2}(M_{11} - M_{ss} + M_{1-1}); \quad d = -\frac{1}{\sqrt{2}\sin\theta}(M_{10} + M_{01}); \quad e = \frac{i}{\sqrt{2}}(M_{10} - M_{01}). \quad (\text{A6})$$

The two-pion exchange box and crossed amplitudes can be written in the form

$$M(\mathbf{k}_f, \mathbf{k}_i) = \langle\langle (G^1 + i\sigma_1 \cdot \mathbf{H}^1)(G^2 + i\sigma_2 \cdot \mathbf{H}^2) \rangle\rangle \quad (\text{A7})$$

where the double brackets indicate integrations over the propagators and the  $G$  and  $\mathbf{H}$  here are related to the corresponding quantities in Section II by the factor  $\frac{m^2}{4\pi E}$  ( $G^1 = \frac{m^2}{4\pi E}G$ ,  $G^2 = \frac{m^2}{4\pi E}G'$ , etc.). With our choice of coordinate system  $G$  and  $H_y$  are even in  $q_y$  while  $H_x$  and  $H_z$  are odd. Any totally odd quantity will integrate to zero and those terms have been dropped in the following expressions. In the remainder of this appendix it is to be understood that each term bilinear in  $G$  and/or  $\mathbf{H}$  is surrounded by double brackets. One has

$$M_{1,1} = G^1 G^2 - H_z^1 H_z^2; \quad M_{s,s} = G^1 G^2 + \mathbf{H}^1 \cdot \mathbf{H}^2; \quad M_{1,-1} = -H_x^1 H_x^2 + H_y^1 H_y^2; \quad (\text{A8})$$

$$M_{0,0} = G^1 G^2 + H_z^1 H_z^2 - H_x^1 H_x^2 - H_y^1 H_y^2; \quad (\text{A9})$$

$$M_{0,1} = \frac{1}{\sqrt{2}}[-H_z^1 H_x^2 - H_x^1 H_z^2 - G^1 H_y^2 - G^2 H_y^1]; \quad (\text{A10})$$

$$M_{1,0} = \frac{1}{\sqrt{2}}[-H_z^1 H_x^2 - H_x^1 H_z^2 + G^1 H_y^2 + G^2 H_y^1]. \quad (\text{A11})$$

From these expressions we can construct the amplitudes as

$$a = G^1 G^2 - H_y^1 H_y^2; \quad b = G^1 G^2 + H_y^2 H_y^2; \quad c = -H_x^1 H_x^2 - H_z^1 H_z^2; \quad (\text{A12})$$

$$d = \frac{1}{\sin \theta} (H_z^1 H_x^2 + H_x^1 H_z^2); \quad e = i(G^1 H_y^2 + G^2 H_y^1). \quad (\text{A13})$$

With the symmetry due to the identical particles

$$a(\theta) \rightarrow a(\theta) - a(\pi - \theta), \quad (\text{A14})$$

$$b(\theta) \rightarrow b(\theta) - c(\pi - \theta) = G^1(\theta)G^2(\theta) + \mathbf{H}^1(\pi - \theta) \cdot \mathbf{H}^2(\pi - \theta), \quad (\text{A15})$$

$$c(\theta) = -b(\pi - \theta), \quad (\text{A16})$$

$$d(\theta) \rightarrow \frac{1}{\sin \theta} [H_z^1(\theta)H_x^2(\theta) + H_x^1(\theta)H_z^2(\theta)H_z^1(\pi - \theta)H_x^2(\pi - \theta) + H_x^1(\pi - \theta)H_z^2(\pi - \theta)], \quad (\text{A17})$$

$$e(\theta) \rightarrow G^1(\theta)H_y^2(\theta) + G^2(\theta)H_y^1(\theta) + G^1(\pi - \theta)H_y^2(\pi - \theta) + G^2(\pi - \theta)H_y^1(\pi - \theta). \quad (\text{A18})$$

At  $90^\circ$

$$a = 0; \quad b = G^1 G^2 + \mathbf{H}^1 \cdot \mathbf{H}^2 = -c; \quad d = 2(H_z^1 H_x^2 + H_x^1 H_z^2); \quad e = 2(G^1 H_y^2 + G^2 H_y^1), \quad (\text{A19})$$

where the quantities are evaluated at  $90^\circ$ .

## APPENDIX B: CALCULATION TECHNIQUE

Consider the interior integrals over  $q$  and  $q_0$  with the integrals over the solid angle to be done at the exterior. We apply two formulae depending on the case. In the integral of the type

$$\int dy \int dx \left\{ \frac{f(x, y)}{[x - x_1(y)][x - x_2(y)]} \right\} \quad (\text{B1})$$

there are two possibilities. If  $x_1$  and  $x_2$  are distinct for all values of  $y$  then we can write the integral as

$$\int dy \int dx \frac{f(x, y) - g(x, y)}{[x - x_1(y)][x - x_2(y)]} + \int dy \int dx \frac{g(x, y)}{[x - x_1(y)][x - x_2(y)]}, \quad (\text{B2})$$

where

$$g(x, y) = \frac{x - x_2(y)}{x_1(y) - x_2(y)} f(x_1(y), y) + \frac{x - x_1(y)}{x_2(y) - x_1(y)} f(x_2(y), y). \quad (\text{B3})$$



The combination  $f(x, y) - g(x, y)$  vanishes at each of the poles so that there is no singularity in the first term. For the second integral we have

$$\int_{-x_0}^{x_0} \frac{g(x, y) dx}{[x - x_1(y)][x - x_2(y)]} = \frac{f(x_1(y), y)}{x_1(y) - x_2(y)} \int_{-x_0}^{x_0} \frac{1}{x - x_1(y)} + \frac{f(x_2(y), y)}{x_2(y) - x_1(y)} \int_{-x_0}^{x_0} \frac{1}{x - x_2(y)} \quad (\text{B4})$$

$$= \frac{f(x_1(y), y)}{x_1(y) - x_2(y)} \left[ \pm i\pi + \ln \left( \frac{x_0 - x_1(y)}{x_0 + x_1(y)} \right) \right] + \frac{f(x_2(y), y)}{x_2(y) - x_1(y)} \left[ \pm i\pi + \ln \left( \frac{x_0 - x_2(y)}{x_0 + x_2(y)} \right) \right]. \quad (\text{B5})$$

For the general case of  $n$  distinct poles

$$\int dy \int \frac{dx f(x, y)}{\prod_{i=1}^n [x - x_i(y)]} = \int dy \int \frac{dx [f(x, y) - g(x, y)]}{\prod_{i=1}^n [x - x_i(y)]} + \int dy \int \frac{dx g(x, y)}{\prod_{i=1}^n [x - x_i(y)]}, \quad (\text{B6})$$

where

$$g(x, y) = \sum_{i=1}^n \frac{\prod_{j \neq i} [x - x_j(y)]}{\prod_{j \neq i} [x_i(y) - x_j(y)]} f(x_i(y), y) \quad (\text{B7})$$

and the second integral is given by

$$\sum_{i=1}^n \frac{f(x_i(y), y)}{\prod_{j \neq i} [x_i(y) - x_j(y)]} \left[ \pm i\pi + \ln \left( \frac{x_0 - x_i(y)}{x_0 + x_i(y)} \right) \right]. \quad (\text{B8})$$

If two poles are not distinct (for some value of  $y$ ) then this method does not work. Instead we may write

$$\int dy \int \frac{dx f(x, y)}{[x - x_1(y)][x - x_2(y)]} = \int dy \frac{1}{x_1(y) - x_2(y)} \int dx f(x, y) \left[ \frac{1}{x - x_1(y)} - \frac{1}{x - x_2(y)} \right]. \quad (\text{B9})$$

Each of these integrals can be done separately and a second singularity has been pushed into the  $y$  integral. In the cases where the pole occurs in quadratic expressions it may be more efficient to take that into account as

$$\int dy \int dx \frac{f(x, y)}{[x^2 - x_1^2(y)][x^2 - x_2^2(y)]} = \int dy \frac{1}{x_1^2(y) - x_2^2(y)} \int dx f(x, y) \left[ \frac{1}{x^2 - x_1^2(y)} - \frac{1}{x^2 - x_2^2(y)} \right]. \quad (\text{B10})$$

### APPENDIX C: INTERPRETATION OF $Z^2$

One can be led to the form of Eq. (76) from the condition given in Eq. (78). Since  $k' = k + q$  (for example) we observe the analogous condition in three dimensions is indicative of the vector cross product and are thus led to consider the four-dimensional version of the cross product. If we define this cross product by the use of a totally antisymmetric 4-component tensor,  $\epsilon_{ijkl}$ , in analogy with the 3-dimensional case, for two vectors (say  $\mathbf{a}$  and  $\mathbf{b}$ ) the result is a tensor

$$T_{ij} = \sum_{0,1,2,3} \epsilon_{ijkl} a_k b_l. \quad (\text{C1})$$

Since this tensor has 6 independent components, it cannot be expressed as an ordinary 4-vector. It is useful to separate the components into two classes: one in which the zero index is free and one in which it is contained in the sum.

$$T_{0j} = \sum_{1,2,3} \epsilon_{0jkl} a_k b_l = [\mathbf{a} \times \mathbf{b}]_j; \quad j = 1, 2, 3, \quad (\text{C2})$$

$$T_{ij} = a_0 b_k - b_0 a_k = [a_0 \mathbf{b} - b_0 \mathbf{a}]_k, \quad i, j, k = 1, 2, 3 \text{ and cyclic.} \quad (\text{C3})$$

Contracting this tensor with itself with the standard metric tensor  $g_{i,j} = g_i \delta_{i,j}$ ;  $g_0 = 1$ ;  $g_i = -1$ ,  $i = 1, 2, 3$  we find

$$\frac{1}{2} \sum g_{ii'} g_{jj'} T_{ij} T_{i'j'} = \frac{1}{2} \sum g_{ii} g_{jj} T_{ij} T_{ij} = (a_0 \mathbf{b} - b_0 \mathbf{a})^2 - (\mathbf{a} \times \mathbf{b})^2 \equiv (a \cdot b)^2 - a^2 b^2. \quad (\text{C4})$$

The last identity may be verified by direct evaluation and has the form used for  $Z^2$  showing that it corresponds to the contraction of a four-dimensional cross product.

- 
- [1] A. Lin et al., Phys. Lett. **74B**, 273 (1978): *Energy dependence of spin-spin forces in  $90^\circ_{cm}$  elastic pp scattering.*
  - [2] T. S. Bhatia et al., Phys. Rev. Lett. **49**, 1135 (1982): *Spin Correlation for pp Elastic scattering at  $\Theta_{c.m.} = \pi/2$  in the Energy Region of Dibaryon Resonances.*
  - [3] E. A. Crosbie et al., Phys. Rev. **D 23**, 600 (1981): *Energy dependence of spin-spin effects in pp elastic scattering at  $90^\circ$  c.m..*
  - [4] G. R. Court et al., Phys. Rev. Lett. **57**, 507 (1986): *Energy Dependence of Spin Effects in  $p_\uparrow + p_\uparrow \rightarrow p + p$ .*
  - [5] D. G. Crabb et al., Phys. Rev. Lett. **41**, 1257 (1978): *Spin dependence of High- $p_\perp^2$  Elastic p-p Scattering.*
  - [6] J. R. O'Fallon et al., Phys. Rev. Lett. **39**, 733 (1977): *Spin-Spin Interaction in High- $p_\perp^2$  Elastic p-p Scattering.*
  - [7] C. W. Akerlof, R. H. Hieber, A. D. Krisch, K. W. Edwards, L. G. Ratner and K. Ruddick, Phys. Rev. **159**, 1138 (1967): *Elastic Proton-Proton scattering at  $90^\circ$  and Structure within the Proton.*
  - [8] R. C. Kammerud, B. B. Brabson, R. R. Crittenden, R. M. Heinz, H. A. Neal, H. W. Paik and R. Sidwell, Phys. Rev. **D 4**, 1309 (1971): *Large-Angle Proton-Proton Elastic Scattering at Intermediate Momenta.*
  - [9] K. Abe, B. A. Barnett, J. H. Goldman, A. T. Laasanen, P. H. Steinberg, G. J. Marmer, D. R. Moffett and E. F. Parker, Phys. Rev. **D 12**, 1 (1975): *Wide-angle differential cross sections for elastic proton-proton scattering in the region of  $\Delta(1236)$  production.*
  - [10] S. J. Brodsky, C. E. Carlson and H. Lipkin, Phys. Rev. **D 20**, 2278 (1979): *Spin effects in large-transverse-momentum exclusive Scattering processes.*
  - [11] G. R. Farrar, S. Gottlieb, D. Sivers and G. H. Thomas, Phys. Rev. **D 20**, 202 (1979): *Constituent description of NN elastic scattering observables at large angles.*
  - [12] G. P. Ramsey and D. Sivers, Phys. Rev. **D 45**, 79 (1992): *Spin observables for  $NN \rightarrow NN$  at large momentum transfer.*
  - [13] G. P. Ramsey and D. Sivers, Phys. Rev. **D 47**, 93 (1993): *Proton-proton elastic spin observables at large  $t$ .*
  - [14] T. E. O. Ericson and M. Rosa-Clot, Nucl. Phys. **A405**, 497 (1983): *The deuteron asymptotic D-state as a probe of the nucleon-nucleon force.*
  - [15] J. L. Friar, B. F. Gibson and G. L. Payne, Phys. Rev. **C 30**, 1084 (1984): *One-pion exchange potential deuteron.*
  - [16] J. L. Ballot and M. R. Robilotta, Phys. Rev. **C 45**, 986 (1992): *Pionic values for deuteron observables*; Phys. Rev. **C 45**, 990 (1992): *Nonpionic effects in deuteron asymptotic observables*; J. L. Ballot, A. M. Eiró and M. R. Robilotta, Phys. Rev. **C 40**, 1459 (1989): *Pions in the deuteron.*
  - [17] W. R. Gibbs and B. Loiseau, Phys. Rev. **C 50**, 2742 (1994): *Neutron-Proton charge exchange.*
  - [18] S. J. Brodsky and G. R. Farrar, Phys. Rev. **D 11**, 1309 (1975): *Scaling laws for large-momentum-transfer processes.*
  - [19] M. Taketani, S. Nakamura and M. Sasaki, Prog. Theor. Phys. **6**, 581 (1951): *On the Method of the Theory of Nuclear Forces.*
  - [20] M. Taketani, S. Machida, and S. Ohnuma, Prog. Theor. Phys. **7**, 45 (1952): *The Meson Theory of Nuclear Forces.*
  - [21] K. A. Brueckner and K. M. Watson, Phys. Rev. **92**, 1023 (1953): *Nuclear Forces in Pseudoscalar Meson Theory.*
  - [22] M. Sugawara and S. Okubo, Phys. Rev. **117**, 605 (1960): *Two-Nucleon Potential from Pion Field Theory with Pseudoscalar Coupling*; *ibid* **117**, 611 (1960): *Two-Nucleon Potential from Pion Field Theory with Pseudovector Coupling.*
  - [23] S. Machida, Prog. Theor. Phys. (Suppl.) **39**, 91 (1967): *Nonstatic Nuclear Potential.*
  - [24] M. H. Partovi and E. L. Lomon, Phys. Rev. **D 2**, 1999 (1970): *Field-Theoretical Nucleon-Nucleon Potential.*
  - [25] W. N. Cottingham, M. Lacombe, B. Loiseau, J.-M. Richard and R. Vinh Mau, Phys. Rev. **D 8**, 800 (1973): *Nucleon-Nucleon Interaction from Pion-Nucleon Phase-Shift Analysis*
  - [26] M. Lacombe, B. Loiseau, J.-M. Richard, R. Vinh Mau, J. Côté, P. Pirès and R. de Tourreil Phys. Rev. **C 21**, 861 (1980): *Parameterization of the Paris NN potential.*
  - [27] J.-M. Richard, *Contribution à l'étude théorique et phénoménologique des forces nucléaires*, Thèse de Doctorat d'État Es-Sciences Physique, Université P. & M. Curie, 19 June 1975.

- [28] J. L. Friar and S. A. Coon, Phys. Rev. C **49**, 1272 (1994): *Non-adiabatic contributions to static two-pion-exchange nuclear potentials.*
- [29] M. R. Robilotta and C. A. da Rocha, Nucl. Phys. **A615**, 391 (1997): *Two-pion-exchange nucleon-nucleon potential model independent features.*
- [30] M. C. M. Rentmeester, R. G. E. Timmermans, J. L. Friar and J. J. de Swart, Phys. Rev. Lett. **82**, 4992 (1999): *Chiral Two-Pion Exchange and Proton-Proton Partial-Wave Analysis.*
- [31] R. P. Feynman Phys. Rev. **76**, 769 (1949): *Space-Time Approach to Quantum Electrodynamics*; see also Jauch and Rohrlich, *The Theory of Photons and Electrons*, Springer-Verlag, New York 1976.
- [32] L. Y. Glozman and D. O. Riska, Phys. Repts. **268**, 264 (1996): *The spectrum of the nucleons and the strange hyperons and chiral dynamics*; L. Y. Glozman, W. Plessas, K. Varga and R. F. Wagenbrunn, Nucl. Phys. **A631**, 469c (1998): *Light and strange baryons in a chiral quark model with Goldstone-boson-exchange interactions*; S. N. Jena, P. Panda, and T. C. Tripathy, Jour. Phys. **G27**, 227 (2001): *Masses of low-lying baryons in the ground states in a power-law potential model with pseudoscalar meson, one-gluon and centre-of-mass corrections*; C. Helminen and D. O. Riska, Phys. Rev. C **58**, 2928 (1998):  *$\pi$ -gluon exchange interaction between constituent quarks*; A. Valcarce, H. Garcilazo and J. Vijande, Phys. Rev. C **72**, 025206 (2005): *Constituent quark model study of light- and strange-baryon spectra*; M. Arima, K. Masutani and T. Sato, Prog. Theor. Phys. Supp. **137**, 169 (2000): *Baryon resonances in a constituent quark model*; H. R. Pang, J. L. Ping, F. Wang and T. Goldman, Phys. Rev. C **65**, 014003 (2002): *Phenomenological study of hadron interaction models.*
- [33] F. Gross and Y. Surya, Phys. Rev. C **47**, 703 (1993): *Unitary, relativistic resonance model for  $\pi N$  scattering.*
- [34] P. F. A. Goudsmit, H. J. Leisi, E. Matsinos, B. L. Birbrair and A. B. Gridnev, Nucl. Phys. **A575**, 673 (1994): *The extended tree-level model for the pion-nucleon interaction.*
- [35] S. Kondratyuk and O. Scholten, Phys. Rev. C **59**, 1070 (1999): *Consistent off-shell vertex and nucleon self-energy.*
- [36] J. Bystricky, F. Lehar and P. Winternitz, J. Phys. **39**, 1 (1978): *Formalism of Nucleon-Nucleon elastic scattering experiments.*
- [37] J. D. Bjorken and S. D. Drell, *Relativistic Quantum Fields* McGraw-Hill, (1965), Chapter 18.
- [38] B.D. Keister and W.N. Polyzou, *Advances in Nuclear Physics*, Volume 20, Ed. J. W. Negele and E.W. Vogt, Plenum Press 1991: *Relativistic Hamiltonian Dynamics in Nuclear and Particle Physics.*
- [39] H.M. Nussenzweig, *Causality and dispersion relations*, Academic Press NY (1972).
- [40] C. M. Maekawa and M. R. Robilotta, Phys. Rev. C **55**, 2675 (1977): *Chiral symmetry: Pion-nucleon interactions in constituent quark models.*
- [41] M. Bozoian, J. C. H. van Doremalen and H. J. Weber, Phys. Lett. **122B**, 138 (1983): *Are There Bound  $A=2$  Hyperon States?*
- [42] S. Nozawa, B. Blankleider and T.-S. H. Lee, Nucl. Phys. **A513**, 459 (1990): *A Dynamical Model of Pion Photoproduction on the Nucleon.*
- [43] H. Haberzettl, C. Bennhold, T. Mart and T. Feuster, Phys. Rev. C **58**, R40 (1998): *Gauge-invariant Tree-level Photoproduction Amplitudes with Form Factors.*
- [44] M. Gourdin, Phys. Rept., **11**, 29 (1974): *Weak and electromagnetic form-factors of hadrons.*
- [45] M. Lissia, M.-C. Chu, J. W. Negele and J. M. Grandy, Nucl. Phys. **A555**, 272 (1993): *Comparison of hadron quark distribution from lattice QCD and the MIT bag model.*
- [46] C. Alexandrou, Ph. de Forcrand and A Tsapalis, Phys. Rev. D **68**, 074504 (2003): *Matter and pseudoscalar densities in lattice QCD.*
- [47] S. A. Coon and M. D. Scadron, Phys. Rev. C **42**, 2256 (1990):  *$\pi NN$  couplings, the  $\pi NN$  form factor and the Goldberger-Treiman discrepancy*; Phys. Rev. C **23**, 1150 (1981): *Goldberger-Treiman discrepancy and the momentum variation of the pion-nucleon form factor and pion decay constant.*
- [48] M. Bolsterli and J. Parmentola, Phys. Rev. D **39**, 1304 (1989): *P-wave pion in the Los Alamos soliton model.*
- [49] G. Ramalho, A. Arriaga and M. T. Peña, Phys. Rev. C **60**, 047001 (1999): *Two-pion exchange and strong form factors in covariant field theories.*
- [50] B. D. Keister and L. S. Kisslinger, Nucl. Phys. **A326**, 445 (1979): *A relativistic study of  $pp \rightarrow d \pi^+$ : Forward scattering*; G. Wolf, Phys. Rev. **182**, 1538 (1969): *Single- and Double-Pion Production by One-Pion Exchange and a Comparison with Experimental Data between 1.6 and 2.6 GeV/c*; H. P. Durr and H. P. Pilkuhn, Nuovo Cim. **40**, 899 (1965): *Kinematical form factors in the peripheral model*; J. Benecke and H. P. Durr, Nuovo Cim. **56**, 269 (1968): *A Relativistic Model for Kinematical Form Factors*; L. Mathelitsch and H. Garcilazo, Phys. Rev. C **33**, 2075 (1986): *Relativistic one-pion exchange potentials.*
- [51] S. Mandelstam, Phys. Rev. **112**, 1344 (1958): *Determination of the Pion-Nucleon Scattering Amplitude from Dispersion Relations and Unitarity. General Theory.*
- [52] G. Höhler,  *$\pi N$  scattering in Landolt-Börnstein*, New Series, Vol. 9b (1983).
- [53] G. E. Brown, A. D. Jackson, *The Nucleon-Nucleon Interaction*, North-Holland/American Elsevier (1976) chap. XIV.
- [54] K. Nishijima, *Fields and particles*, W. A. Benjamin Inc. 1969, pp 419-421.
- [55] R. E. Cutkosky, J. Math. Phys. **1**, 429 (1960): *Singularities and Discontinuities of Feynman Amplitudes.*
- [56] H. Zytnecki, *Paramètre de corrélation de spin proton-proton à  $90^\circ$  jusqu'à 12 GeV/c et échange de deux pions à*

*l'aide des relations de dispersion*, Rapport de stage de D.E.A. de Physique Quantique, Uni. P. & M. Curie, Paris, <http://lpnhe-theorie.in2p3.fr/TH-Rapp.html>.

- [57] SAID program at <http://gwdac.phys.gwu.edu>; R. A. Arndt, I. I Strakovsky and R. L. Workman, Phys. Rev. C **62**, 034005 (2000): *Nucleon Nucleon Elastic Scattering to 3 GeV*.
- [58] J. Bystricky, C. Lechanoine-LeLuc and F. Lehar, Eur. Phys. J. **C4**, 607 (1998): *Direct reconstruction of pp elastic scattering amplitudes and phase shift analyses at fixed energies from 1.80 to 2.70 GeV*.
- [59] N. Ghahramany, G. Forozani, Phys. Rev. C **61**, 064004 (2000): *Direct reconstruction of pp elastic scattering amplitudes at 1.8 and 2.1 GeV*.
- [60] R. D. Amado and R. M. Woloshyn, Phys. Lett. **62B**, 253 (1976): *Momentum distribution in the nucleus*.
- [61] P. Jain, B. Pire and J. P. Ralston, Phys. Rept. **271**, 67 (1996): *Quantum color transparency and nuclear filtering*.
- [62] A. S. Carroll et al. Phys. Rev. Lett. **61**, 1698 (1988): *Nuclear Transparency to Large-Angle pp Elastic Scattering*.